MOBILE SLEEP APNEA DETECTION AND MONITORING BASED ON THERMOCOUPLE AND PULSE OXIMETER SENSORS

A THESIS SUBMITTED TO
THE GRADUATE SCHOOL OF NATURAL AND APPLIED SCIENCES
OF
MIDDLE EAST TECHNICAL UNIVERSITY

BY

DUYGU DEMİRKOL ÇAKMAK

IN PARTIAL FULFILLMENT OF THE REQUIREMENTS
FOR
THE DEGREE OF MASTER OF SCIENCE
IN
ELECTRICAL AND ELECTRONICS ENGINEERING

MAY 2018

Approval of the thesis:

MOBILE SLEEP APNEA DETECTION and MONITORING BASED ON THERMOCOUPLE AND PULSE OXIMETER SENSORS

submitted by **DUYGU DEMİRKOL ÇAKMAK** in partial fulfillment of the requirements for the degree of **Master of Science in Electrical and Electronics Engineering Department, Middle East Technical University** by,

Prof. Dr. Halil Kalıpçılar _____
Dean**,** Graduate School of **Natural and Applied Sciences**

Prof. Dr. Tolga Çiloğlu _____
Head of Department, **Electrical and Electronics Engineering**

Prof. Dr. B. Murat Eyüboğlu _____
Supervisor, **Electrical and Electronics Engineering Dept., METU**

Examining Committee Members:

Prof. Dr. Nevzat Güneri Gencer _____
Electrical and Electronics Engineering Dept., METU

Prof. Dr. B. Murat Eyüboğlu _____
Electrical and Electronics Engineering Dept., METU

Assoc. Prof. Dr. Yeşim Serinağaoğlu Doğrusöz _____
Electrical and Electronics Engineering Dept., METU

Assoc. Prof. Dr. Barış Bayram _____
Electrical and Electronics Engineering Dept., METU

Asst. Prof. Dr. Gökhan Şengül _____
Computer Engineering Dept., Atılım University

Date: 23.05.2018

I hereby declare that all information in this document has been obtained and presented in accordance with academic rules and ethical conduct. I also declare that, as required by these rules and conduct, I have fully cited and referenced all material and results that are not original to this work.

Name, Last name: Duygu DEMİRKOL ÇAKMAK

Signature:

ABSTRACT

MOBILE SLEEP APNEA DETECTION and MONITORING BASED ON THERMOCOUPLE and PULSE OXIMETER SENSORS

Demirkol Çakmak, Duygu
M.S., Department of Electrical and Electronics Engineering
Supervisor: Prof. Dr. B. Murat Eyüboğlu

May 2018, 87 Pages

Sleep apnea syndrome is becoming a prevalent disease for both adults and children. It is described as the cessation of breath for at least 10 seconds during sleep. Detecting sleep apnea is considered as a troublesome and time-consuming method, which requires the patients to stay one or more nights in dedicated sleep disorder rooms with sensors physically attached to their body. Undiagnosed, thereby untreated, sleep apnea patients are under high risk of hypertension, heart attack, accidental injuries through fatigue and sleeplessness. In this project, a portable, low cost and user friendly device to detect sleep apnea which is able to share the necessary information to the patients and doctors during the duration of the whole sleep cycle is developed. To this end, nasal and oral respiratory information is obtained with utilizing thermocouple and oxygen saturation in the blood is obtained with utilizing pulse oximeter. An analog electronic circuit is designed to readout thermocouple and pulse oximeter signals. According to the collected respiratory and pulse oximetry signals, sleep apnea is detected in real time by a software implemented into an ARM based processor. An Android mobile application is developed to record and display the oxygen saturation, heart rate and respiratory signal data during sleep. Communication between ARM based processor and mobile application is established via Bluetooth interface to reduce cabling on the patient.

The experimental results gathered from five subjects show that number of sleep apnea can be detected with 100% accuracy, heart rate and SpO_2 can be calculated with approximately 99% accuracy.

Keywords: Sleep apnea, thermocouple, pulse oximeter, mobile application, Bluetooth

ÖZ

ISIL ÇİFT ve OKSIMETRE SENSÖRLERİNE DAYALI TAŞINABİLİR UYKU APNESİ SAPTANMASI ve İZLENMESİ

Demirkol Çakmak, Duygu
Yüksek Lisans, Elektrik ve Elektronik Mühendisliği Bölümü
Tez Yöneticisi: Prof. Dr. B. Murat Eyüboğlu

Mayıs 2018, 87 Sayfa

Uyku apnesi sendromu hem çocuklarda hem de yetişkinlerde yaygın görülen bir hastalık olmaya başlamıştır. Uyku apnesi; uyku esnasında nefesin en az 10 saniye süre ile kesilmesi olarak tanımlanır. Uyku apnesinin tespiti, hastaların fiziksel olarak vücutlarına bağlanmış sensörlerle birlikte, özel uyku bozukluğu odalarında bir ya da bir kaç gece kalmalarını gerektiren, zahmetli ve zaman alıcı bir yöntem olarak nitelendirilir. Hastalıkları tespit edilememiş, dolayısıyla tedavi edilememiş uyku apnesi hastaları yüksek tansiyon, kalp krizi ile yorgunluk ve uykusuzluktan kaynaklı kazara yaralanma riski altındadır. Bu tezde, uyku apnesinin tespiti için, tüm uyku döngüsü süresince, hastalara ve doktorlara gerekli bilgileri paylaşabilen, taşınabilir, düşük maliyetli ve kullanıcı dostu bir cihaz geliştirilmiştir. Bu amaçla, ısıl çift kullanılarak ağızdan ve burundan solunum sinyali, oksimetre kullanılarak ise kandaki oksijen saturasyonu elde edilmiştir. Isıl çift ve oksimetre sinyallerini okumak için analog devre tasarlanmıştır. Solunum ve oksimetre sinyallerine göre, ARM tabanlı bir işlemci üzerinde çalışan yazılım ile gerçek zamanlı uyku apnesi tespiti yapılmıştır. Oksijen saturasyonu, nabız ile solunum sinyalinin uyku boyunca gözlemlenmesi ve kayıt edilmesi için Android mobil uygulama geliştirilmiştir. ARM tabanlı işlemci ile mobil uygulama arasındaki iletişim hasta üzerindeki kablo yoğunluğunu azaltmak için Bluetooth ile sağlanmıştır. Beş kişiden elde edilen deney

sonuçları, uyku apnesinin %100 doğrulukla tespit edilebileceğini, nabzın ve SpO_2'nin ise yaklaşık %99 doğrulukla hesaplanabileceğini göstermektedir.

Anahtar Kelimeler: Uyku apnesi, ısıl çiftler, oksimetre, mobil uygulama, Bluetooth

To my lovely family…

ACKNOWLEDGEMENTS

I would like to express my deepest gratitude to my supervisor Prof. Dr. Murat Eyüboğlu for his invaluable comments, support, leadership and patience throughout the entire research.

I would like to thank to my biomedical lab mates in METU and my colleagues in ROKETSAN for their encouragement and support. I would like to express my special thanks to Seyit Tunç and Ulaş Kürüm for the helpful suggestions, editing and advises. The technical discussions we made with them about the thesis are very significant for me.

Also, I would like to express my sincere thanks to Yeşim Günhan, Derya Ünsal and Bağış Altınöz for their endless support and friendship. I know that they will always stand by me in the good and bad times.

In addition, I would like to express my gratefulness to Mehmet Caner İşmar and Kadir Güngör who helped me with the mechanical drawing of the system and directed me with innovative ideas on mechanical design.

I would like to express my greatest appreciation to Burkay Sucu who encourage me all the times and help me in the hardest times during the thesis work.

Finally, I would like to thank to my lovely big family for their endless love, understanding, complete support and motivation in every moment of my life. My parents, Seher Demirkol and Hüseyin Eren Demirkol, who are always strong and cheerful, are the reason why I can get over the troubled and bad days. My dear sisters Özgün Demirkol Soyarslan and Eren Kırık are the only people that I can consult and trust in every issue. Alparslan Kırık and Celal Soyarslan, even when they are far away, help me whenever I needed. Luckily, I have my dear husband Caner Çakmak who is always patient, self-sacrificing and optimistic during the distressed days of my thesis work. Without his priceless love and attention, I would not achieve this success.

TABLE OF CONTENTS

LIST OF TABLES

TABLES

LIST OF FIGURES

FIGURES

LIST OF ABBREVIATIONS

AASM: American Academy of Sleep Medicine

ADC: Analog to Digital Converter

AI: Apnea Index

bpm: beats per minute

CMOS: Complementary Metal-Oxide Semiconductor

CMRR: Common Mode Rejection Ratio

CSA: Central Sleep Apnea

CPAP: Continuous Positive Airway Pressure

dB: decibel

ECG: Electrocardiogram

EEG: Electroencephalography

EOG: Electrooculogram

F: Female

FN: False Negatives

FP: False Positives

H: hour

FFT: Fast Fourier Transform

IA: Instrumentation Amplifier

ISA: Instrument Society of America

IR: Infrared

LCD: Liquid Crystal Display

LED: Light Emitting Diode

LPF: Low Pass Filter

LPKF: Leiterplatten Kopier Fräsen (translated as circuit board copy milling)

M: Male

OSA: Obstructive Sleep Apnea

PCB: Printed Circuit Board

PPG: Photoplethysmogram

PSG: Polysomnography

R: Red

SaO_2: Functional Oxygen Saturation in the Blood

SMT: Surface Mount Technology

SpO_2: Oxygen Saturation in the Blood

TN: True Negatives

TP: True Positives

Vpp: Peak to Peak Voltage

Y(f): FFT of y(t) signal

CHAPTER 1

INTRODUCTION

Just like eating and breathing, sleeping is a vital necessity for all living organisms. The quality of sleep effects people's mental health, physical health, quality of life and safety. Mental health is related to brain activity and sleep helps one's brain work properly. In case of sleep deficiency, people may have trouble in learning, making decisions, problem solving, paying attention, controlling emotions and behaviour. On the other hand, sleep plays an important role for physical side of health by repairing heart and blood vessels. Besides the increased risk of heart disease, kidney disease, high blood pressure and stroke, sleep deficiency is also linked to obesity, imbalance of hormones and weak immune system [1].

Sleep apnea is a serious health problem which can even be fatal [2]. Therefore, detection of sleep apnea is significant for patients. In this thesis, a portable and efficient module for detecting and monitoring sleep apnea during the whole sleep cycle has been developed. Using this portable module, respiration signal is obtained by a thermocouple; heart rate and oxygen saturation level are obtained with utilizing a pulse oximeter. The module also includes a user friendly mobile application for monitoring the related physiological data, and sharing it with a doctor or specialist.

1.1 Anatomy and Physiology of the Respiration System

The aim of the respiration system is exchanging gas by getting oxygen from external environment and expelling carbon dioxide into the air [3]. Oxygen is the primary need of all living cells in the body to function. But most of the tissue cells stay far away from the inhaled air to use it directly. Therefore, oxygen should be transferred to the bloodstream to provide the required oxygen to every cell in the body.

Blood circulation repeats during every breath. In inhalation, oxygen first enters the nose or mouth then travels through the larynx and trachea that splits into two bronchi. Each bronchus contains bronchial tubes as smaller branches. These bronchial tubes consist of many pathways inside the lung and end with tiny sacs called alveoli. Oxygen diffusion to the lung capillary and carbon dioxide flow to bronchial pathways by the names of gas exchange takes place at the alveoli. After the gas exchange, exhalation begins and this time CO_2 starts to travel from bronchial pathways to the air through nose or mouth. Anatomically, the respiratory system can be divided into two parts as the upper tract which includes the nose, mouth, pharynx, larynx and the lower respiratory tract which includes trachea, bronchi, bronchiole, alveolar duct, alveoli. These tracts of respiratory system are shown in Figure 1.

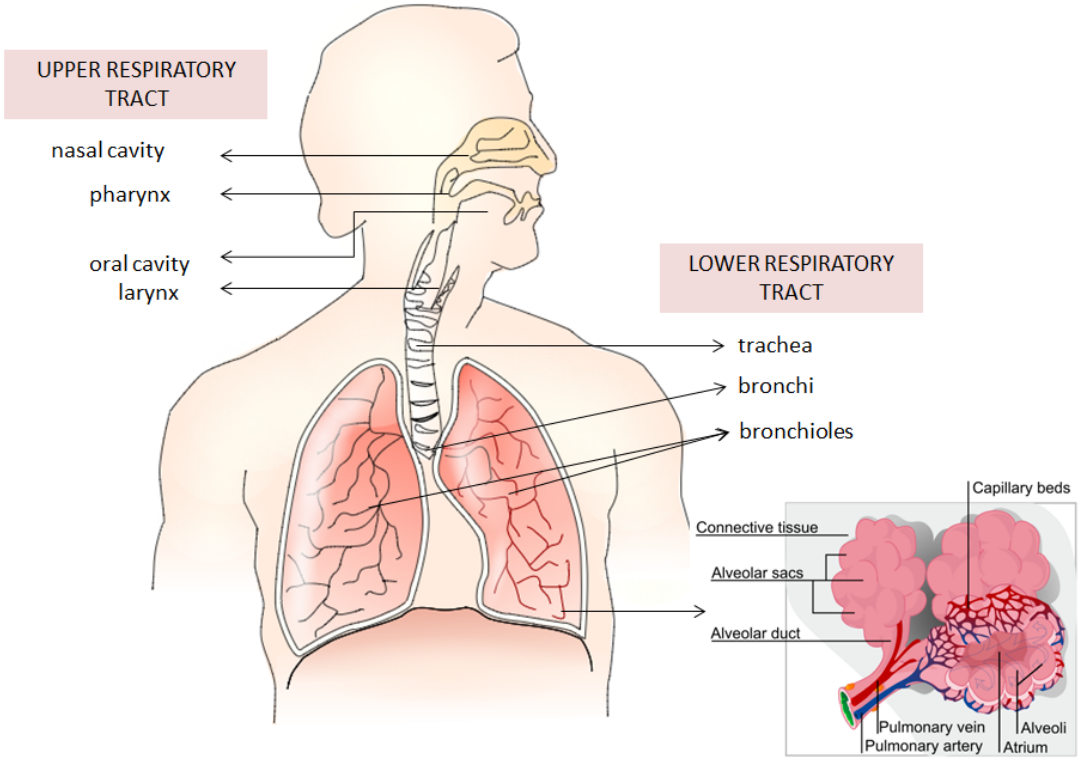

Figure 1 Upper and lower respiratory tracts from oral cavity to the alveoli [4] [5]

Ventilation is an involuntary, rhythmic process which is controlled by respiratory neurons in the brain stem and describes the air movement in and out of the lungs [6].

Ventilation mechanics are based on the principle of air flow from high pressure areas to low pressure areas. If the thoracic cavity expands due to the contraction of the intercostal muscles, pectoral muscles, and the diaphragm, air flows to the lungs, while the atmospheric pressure is higher than the pressure inside the lungs. This process is termed as inspiration. In contrary, according to the relaxation of the intercostal muscles and the diaphragm, lungs volume decreases and thoracic cavity pressure increases. If the pressure in the lungs is higher than the atmospheric pressure, air flows out of the lungs. This process is termed as expiration.

Pleural and alveolar pressure changes caused by the lung volume changes during inspiration and expiration are shown in Figure 2. Pleural pressure is the fluid pressure which occurs between the lung pleura and the chest wall pleura. Alveolar pressure shows the air pressure inside the lung alveoli [7]. Difference between the pleural pressure and the alveolar pressure gives transpulmonary pressure.

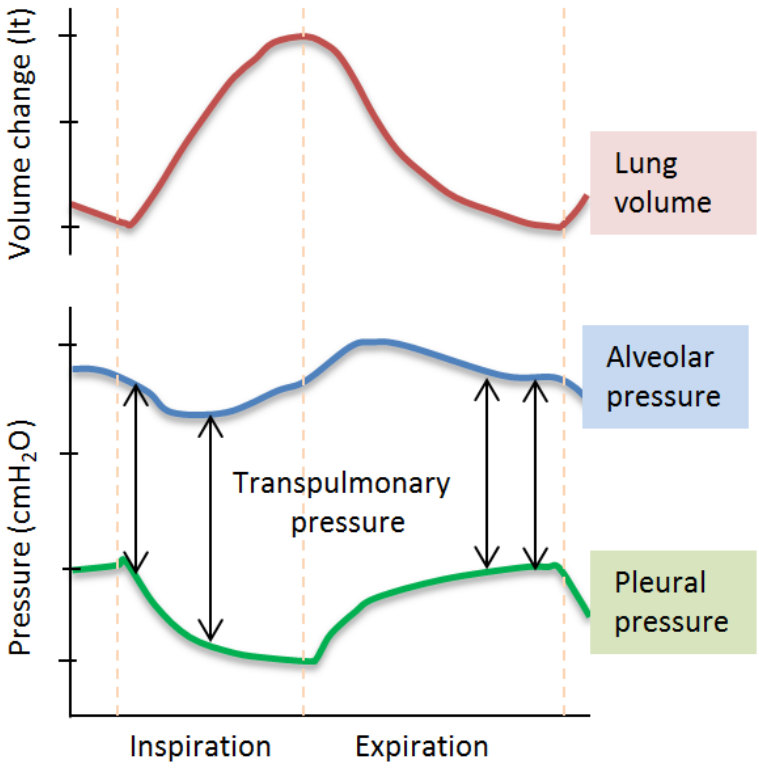

Figure 2 Visualization of alveolar and pleural pressure changes during inspiration and expiration

1.2 Sleep Apnea and Polysomnography

The word “apnea” is a Greek originated term which means “without breath” [8]. Sleep apnea is a common breathing disorder which is the cessation of respiration longer than 10 seconds during sleep [9]. There are three apnea types which are obstructive, central and mixed. Obstructive sleep apnea (OSA) is the most common type which occurs when there is a partial or complete collapse of the upper air path by the soft tissue in the rear of the throat [10] [11]. This means there is no air flow to the lungs despite the effort of chest and brain. If the breathing control muscles could not get the proper signal due to the brain inactivity, central sleep apnea (CSA) occurs [12]. Therefore, CSA is usually associated with instability of the feedback mechanism which controls respiration [13]. In contrast to OSA, no respiratory effort is observed in the case of CSA during the cessations of breath. Mixed sleep apnea, as the name implies, is the mixed of OSA and CSA. For example, it starts with OSA and ends with CSA.

People with untreated sleep apnea may experience the cessation of breath more than hundreds of times and often the cessation takes longer than one minute during the sleep cycle [8]. Some usual nocturnal symptoms of sleep apnea are nocturia and insomnia. Common daytime symptoms of sleep apnea are fatigue or tiredness, daytime sleepiness, cognitive deficits, morning headache, dry or sore throat [14] [15]. Sleep apnea is a remarkable public health issue all over the world. Most of the patients do not realize the disorder, because they are not fully awake after the cessation of breath.

The gold standard for sleep apnea diagnosis is polysomnography (PSG), but it is expensive and inconvenient for the patients [1] [16]. During polysomnography exam, patient should stay overnight in a specially equipped sleep laboratory and the device simultaneously records several physiological parameters such as electroencephalogram (EEG), electrooculogram (EOG), electrocardiogram (ECG), respiratory activity, blood oxygen levels (SpO_2), body motion etc. Because of this troublesome, costly and labor intensive method, great majority of the sleep apnea

patients remain undiagnosed [17]. Studies promote that 93% of women and 82% of men with sleep apnea syndrome have not been clinically diagnosed [18]. Undiagnosed thereby untreated sleep apnea patients are under high risk of hypertension, memory problems, heart attack, weight gain, impotence, headaches and traffic or job accident through tiredness and sleeplessness [19] [20].

When diagnosed, there are several treatment options for sleep apnea like taking surgical operations to the airway or using continuous positive airway pressure (CPAP) [10] [21].

1.3 Computer Aided Sleep Apnea Detection

There are lots of studies based on automatic detection of sleep apnea due to the fact that taking fully equipped PSG test is time consuming, expensive, labor intensive and troublesome for the patients. Having a simplified, reliable and convenient diagnosis or monitoring of sleep apnea without PSG test has become remarkable on the last years. A variety of different sensors for respiration detection, blood oxygen saturation, cardiac or brain activity, body motion etc. are used in the sleep apnea detection works.

N. Oliver and F. Flores-Mangas developed a device called HealthGear [22] which is a wearable, real-time monitoring system and uses pulse oximeter. HealthGear includes three main parts: pulse oximetry sensor, a data transmission module and a mobile phone. This system uses only SpO_2 information as physiological data and transmits the data wirelessly via Bluetooth to a mobile phone and use the data transmission module to analyse, record and detect sleep apnea. Similar with the HealthGear, A. Garde et al. [23] proposed a portable device named as Phone Oximeter, which can be integrated to a smartphone. Sleep apnea analysis is realized by combining blood oxygen saturation and heart rate variability (HRV).

Video processing techniques are also used for sleep apnea detection from body movement, but it is expensive due to the need for the tremendous amount of signal processing tasks. Therefore, analysis of the collected data to detect abnormal breathing and sleep apnea is usually done offline [24] [25].

Lots of studies show that sleep apnea can be detected by the fluctuations on ECG signal because of cyclic variations of a heartbeat. G. Sannino et al. [26], use single channel ECG for detection and real-time monitoring of sleep apnea. Set of rules are extracted offline automatically containing Heart Rate Variability (HRV) parameters. G. Surrel and S. Murali [27] used frequency based algorithms to detect sleep apnea based on ECG recordings. Their system is also wearable and serves real-time screening. Besides, time varying auto regressive models and wavelet transform are also used to detect sleep apnea based of ECG recordings without portable devices and offline algorithms [28] [29].

There are home sleep tests using accelerometer in order to examine sleep apnea from body position [30] [31]. An accelerometer is usually placed on the chest or abdomen to determine the sleeping posture. By this way, spending a long period of time sleeping in supine position can be prevented. In addition to accelerometers, abdominal strain gauges for thoracic movements are also used in some home sleep devices [32] [33].

Since obstructive sleep apnea occurs by blocking the airway's airflow, snoring may happen due to the vibration of soft tissues in the upper airway [34]. This leads to studies about OSA detection based on breathing sounds or snoring [35].

J. Jin and E. Sanchez-Sinencio [16] use pressure sensor based on micro electro mechanical systems (MEMS) for measuring the patient's nasal air flow. Using MEMS technology serves compact and low profile solutions for sensors which makes patients comfortable, but the system needs a PC to run algorithms.

Sechang et al. [36] suggest a wireless sleep apnea monitoring system by using more than one different biomedical signal as ECG, body position, nasal airflow, abdomen and chest efforts and oxygen saturation. The system uses wireless transmitter to send the measured signals to the host computer. Matlab software environment is used for sleep apnea detection algorithms, therefore the system is real time but not portable.

According to the literature review, all computer aided sleep apnea detection systems have individual drawbacks. Some of the studies do not serve real-time detection or are bulky and not portable, some of the studies do not have any recording capability and are only used for monitoring. Some studies need a medical specialist to annotate the sleep stages before performing the algorithm. Furthermore, the method of diagnosing sleep apnea must be appropriate to The American Academy of Sleep Medicine (AASM) Manual. According to the revised version of AASM Manual for the Scoring of Sleep and Associated Events in 2012, the recommended sensor to score apnea in diagnostic study is oronasal thermal airflow sensor [37]. Therefore, in this study a thermocouple is used as the oronasal thermal sensor and the pulse oximeter is used as an alternative. An ARM based processor is used to process respiration and oxygen saturation signals and send the data to the Android mobile application over Bluetooth communication. The system also has the ability to send the whole night records to the doctor or the related people via e-mail or any other social account. If there is a case where the cessation takes longer than 30 seconds during the sleep, alarm is rung to wake up the patient or the bed partner to avoid the fatal risks.

1.4 Objectives of the Study

The contributions of this thesis to the apnea studies are the following:

- Obtaining the respiration signal, which is necessary for sleep apnea detection, from a low cost thermocouple
- Recording the patient respiration signal, heart rate and SpO_2 information of the whole night sleep accurately, obtaining the data in patient's home, using a portable device

The following topics are covered in this thesis:

- Recording the respiration and PPG signal of patients with a thermocouple and a pulse oximeter simultaneously
- Implementing threshold crossing point algorithm to detect apneic attacks and implementing peak detection algorithm to calculate SpO_2 and heart rate in real time
- Finding the AI of the whole night sleep
- Calibrating the pulse oximeter in order to calculate SpO_2
- Sending the necessary information to the doctor or the related people over wireless Bluetooth interface
- Warn the patient or bed partner in case of the apnea which lasts for longer than 30 seconds
- A user friendly Android mobile interface to record, display and share the important data
- Bluetooth communication between mobile device and the sleep apnea detecting device

1.5 Outline of the Thesis

In Chapter 1, anatomical and physiological side of the respiration is explained. Sleep apnea definition, types, diagnosing and treatment methods are detailed. Literature search about the computer aided sleep apnea detection is also given in this chapter.

In Chapter 2, working principles of the sensors used in sleep apnea detection and monitoring is detailed. Mathematical backgrounds of the pulse oximeter and the thermocouple are provided in this chapter.

In Chapter 3, designed sleep apnea detection and monitoring system is described briefly. Specifications of the used sensors, analog hardware unit, Bluetooth communication between ARM processor and the device, ARM software design and the algorithms are shared in this chapter.

Chapter 4 provides the PCB design, manufacturing processes and 3D prototype of the sleep apnea detection device. CMRR measurement of the instrumentation amplifiers and the output signals of the designed analog circuits are also shown in this chapter.

Experimentation set up which includes creating test database and the calibration of pulse oximeter is provided in Chapter 5.

Finally, in Chapter 6, summary of the whole study in this thesis is given. Results of the experimentation and the discussions are also outlined in this chapter.

CHAPTER 2

THEORY

2.1 Introduction

Pulse oximeter is a medical device for non-invasive measuring of arterial oxygen saturation in the blood [6]. The history of pulse oximetry studies is very old. The first attempt to improve pulse oximeter is made by a German physician Karl Matthes in 1935 [38]. It is developed over time and commercialized by Nellcor in 1983. Nowadays, it is recognized worldwide as the standard of care in anesthesiology and used almost everywhere from emergency, home care, sleep laboraties to birth and veterinary medicine [6]. In this thesis, it is used to record of oxygen saturation in the blood and heart rate of the patient to have alternative information for sleep apnea detection.

Thermocouple is an electronic device composed of two different electrical conductors joined with electrical junctions at different temperatures. Based on thermocoelectric effect, a temperature dependent voltage occurs as an output of thermocouple. Thermocouples have variety of application areas such as temperature sensors in thermostats or a flame sensors in safety devices. In addition they are also used in kilns, gas turbine exhaust, diesel engines and other industrial processes. In this thesis, thermocouple is used to obtain respiration with utilizing the temperature changes during breathing. According to the respiration changes sleep apnea is detected.

In this chapter, detailed working principle of the sensors which are used in this thesis is provided.

2.2 Pulse Oximetry Working Principle

2.2.1 Beer-Lambert's Law

The theory behind the pulse oximetry is based on Beer-Lambert's Law. According to the Beer-Lamber's law; concentration of an absorbing substance in a solution can be determined from the intensity of light, transmitted through the absorbing material [39]. Relation between the intensity of transmitted light (I) and the incident light intensity (I_0) can be expressed as:

$$I = I_0 \times e^{-\varepsilon(\lambda)cd} \tag{2.1}$$

In Equation 2.1, $\varepsilon(\lambda)$ is the wavelength dependent extinction coefficient, c is the concentration of the tissue or absorber and d is the optical path length. The transmittance (T) factor of light travelling through a medium is stated by using transmitted and incident light.

$$T = \frac{I}{I_0} = e^{-\varepsilon(\lambda)cd} \tag{2.2}$$

Absorbance (A) can be found from transmittance by taking the natural logarithm, because they are directly related.

$$A = -lnT = \varepsilon(\lambda)cd \tag{2.3}$$

If there is more than one substance absorbs light in the medium, Beer-Lambert's law is still valid and total absorbance (A_t) is calculated with the contribution of every independent absorbance coefficients.

$$A_t = \varepsilon_1(\lambda)c_1d_1 + \varepsilon_2(\lambda)c_2d_2 + \cdots + \varepsilon_n(\lambda)c_nd_n = \sum_{i=1}^{n} \varepsilon_i c_i d_i \tag{2.4}$$

In Equation 2.4, i and d_i is the optical path length through the absorbing substance, which differs from substance to substance in the medium. Therefore, by using Beer-Lambert's law, unknown concentrations of n different absorbing substances in a homogeneous medium can be calculated. But the light absorbance with different wavelengths and the extinction coefficients of the substances should be known.

2.2.2 Hemoglobin Extinction Coefficients

The main light absorber in the blood is the hemoglobin. The absorbing characteristic of hemoglobin changes according to the chemical transportation and the wavelength of the incident light. There are two hemoglobin types as functional and dysfunctional hemoglobins. Dysfunctional hemoglobins are not responsible for transporting oxygen to the tissues. The four most common dysfunctional hemoglobins are methemoglobin (MetHb), carboxyhemoglobin (COHb), sulfhemoglobin, and carboxysulfhemoglobin. In contrast, functional hemoglobins' main responsibility is the transportation of oxygen to the pulmonary capillaries and releasing it in the systemic capillaries. A hemoglobin which is fully saturated with oxygen is called oxyhemoglobin (HbO_2). In contrast, deoxygenated haemoglobin, also called reduced hemoglobin (Hb), is not fully saturated with oxygen [6].

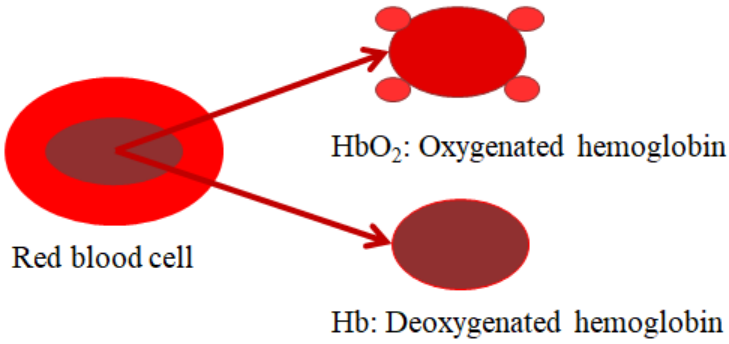

Figure 3 Functional hemoglobin types

The functional hemoglobin saturation is also equivalent with functional arterial oxygen saturation (functional SO_2 or S_aO_2) and it is stated as;

$$SO_2 = \frac{HbO_2}{HbO_2 + Hb} \times 100\% = \frac{c_{HbO_2}}{c_{HbO_2} + c_{Hb}} \times 100\% \quad 2.5$$

Oxygenated hemoglobin (HbO_2) is brighter red which absorbs more infrared light and the deoxygenated hemoglobin (Hb) is darker red which implies that it absorbs more red lights [6]. This change in colour is lead to design pulse oximetry to measure oxygen saturation. According to the absorbation coefficients of red and infrared light in the oxygenated and deoxygenated blood, transmitted signal amplitude changes. A pulse oximeter uses two LEDs with 660 and 940 nm wavelengths by shining them sequentially through a tissue bed like finger or earlobe and measures the transmitted light signal to calculate oxygen saturation in the blood.

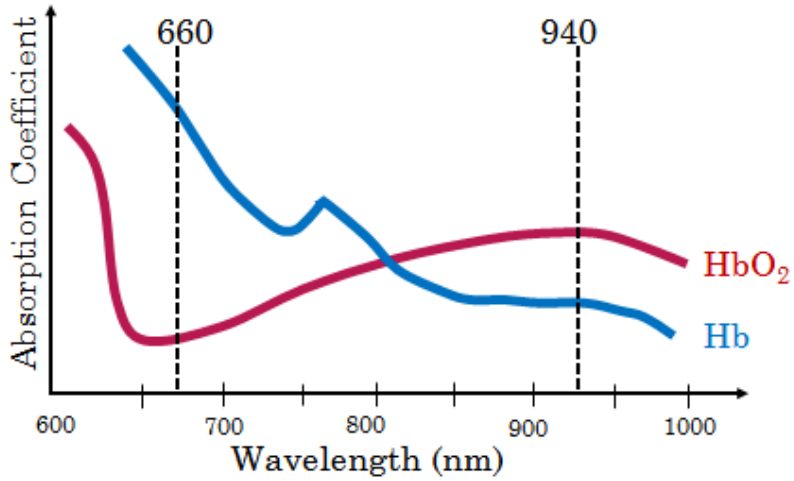

Figure 4 Absorption coefficients of functional hemoglobin species at the wavelengths of interest in pulse oximetry

Equation 2.5 can be reformulated by using the concentrations of oxygenated hemoglobin (c_{HbO_2}) and reduced hemoglobin (c_{Hb}) as a function of SO_2;

$$c_{HbO_2} = SO_2(c_{HbO_2} + c_{Hb}) \quad 2.6$$

$$c_{Hb} = (1 - SO_2)(c_{HbO_2} + c_{Hb})$$

From Equation 2.4, total absorbance A_t can be described just containing oxygenated and deoxygenated hemoglobin as absorbing surstances;

$$A_t = \varepsilon_{HbO_2}(\lambda) c_{HbO_2} d_{HbO_2} + \varepsilon_{Hb}(\lambda) c_{Hb} d_{Hb} \quad 2.7$$

Assuming that the optical path length d is the same for both oxygenated and deoxygenated hemoglobin, Equation 2.8 can be derived by using Equation 2.6 and 2.7.

$$A_t = \left[\varepsilon_{HbO_2}(\lambda) SO_2 + \varepsilon_{Hb}(\lambda)(1 - SO_2)\right](c_{Hb} + c_{HbO_2}) d \quad 2.8$$

Equation 2.8 shows that, total absorbance A_t can be expressed with all known parameters as concentrations of hemoglobin, the extinction coefficients of hemoglobin and the optical path length. Because of the most commonly used wavelengths are 660 and 940nm, extinction coefficient values of adult oxygenated (ε_{Hb}) and deoxygenated hemoglobin (ε_{HbO_2}) values have been measured by Zijlstra et al (1991) and shown in Table 1 [40].

Table 1 Extinction coefficients of oxygenated and deoxygenated hemoglobin in adults at the wavelengths of 660 nm and 940 nm

Wavelength, nm	Extinction coefficient, L $mmol^{-1}cm^{-1}$	
	Hb	HbO_2
660	0.81	0.08
940	0.18	0.29

2.2.3 Pulsation of the Blood

Some part of the transmitted light through the tissue is absorbed by different absorbing subtances mostly the skin, bone, muscle, arterial, and venous blood [41]. The arteries carry more blood during systole than during diastole, this leads to increase pressure and the diameter. Therefore, during systole the absorbance of light in tissues is also increased in arteries. There is not any effect like this in the veins. According to the systole and diastole, blood pressure changes and this makes arteries to have a pulsatile shape [6]. Pulse oximeters use this principle to split the light absorbances into a pulsatile component (AC) and a constant or nonpulsatile component (DC) which is shown in Figure 5 [42].

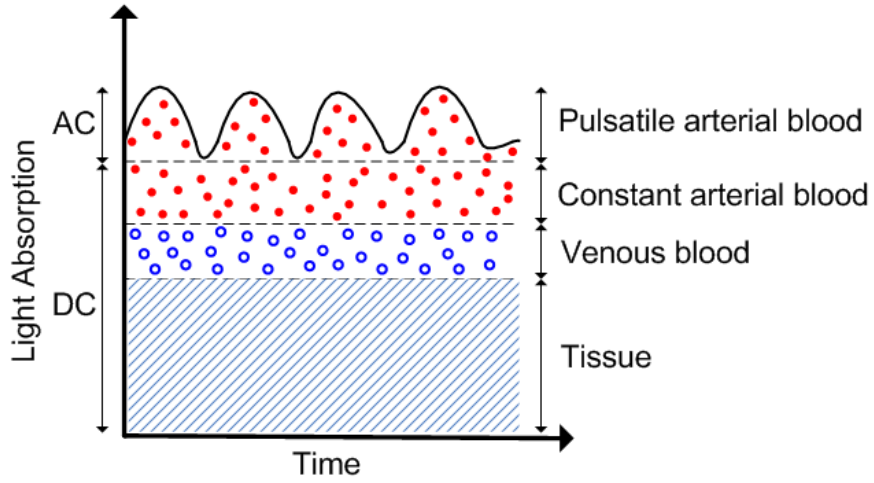

Figure 5 Light absorption through living tissue

The light intensity during diastole is high because the optical path length is low. The presented absorbers during diastole are DC components as shown in Figure 5. Therefore intensity during diastole can be expressed as;

$$I_H = I_0\, e^{-\varepsilon_{DC}(\lambda)c_{DC}d_{DC}}\, e^{-[\varepsilon_{Hb}(\lambda)c_{Hb}+\varepsilon_{HbO_2}(\lambda)c_{HbO_2}]d_{min}} \quad 2.9$$

Where, $\varepsilon_{DC}(\lambda)$, c_{DC}, and d_{DC} are nonpulsatile parameters, I_0 is the incident light and I_H is the transmitted light in diastole. During systole optical path length becomes maximum and the transmitted light (I_L) reaches the low peak and can be expressed as;

$$I_L = I_0\, e^{-\varepsilon_{DC}(\lambda)c_{DC}d_{DC}}\, e^{-[\varepsilon_{Hb}(\lambda)c_{Hb}+\varepsilon_{HbO_2}(\lambda)c_{HbO_2}]d_{max}} \qquad 2.10$$

The arriving light to the photodedector is a function of the diameter d and in cardiac cycle, from diastole to systole, optical path diameter changes from d_{min} to d_{max}. By substituting d with $d_{min} + \Delta d$ the following Beer-Lambert equation is found;

$$I = I_H\, e^{-[\varepsilon_{Hb}(\lambda)c_{Hb}+\varepsilon_{HbO_2}(\lambda)c_{HbO_2}]\Delta d} \qquad 2.11$$

The minimum (I_L) and the maximum (I_H) level of transmittance light due to the minimum optical path length (d_{min}) in diastole and the maximum optical path length (d_{max}) in systole is shown in a simplified model in Figure 6.

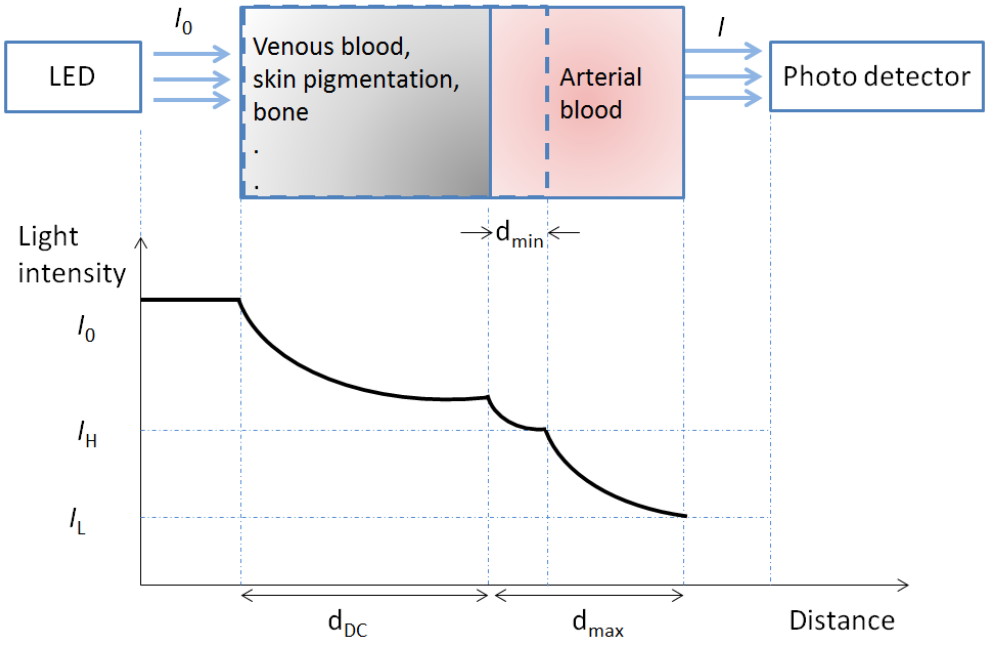

Figure 6 Simplified model of Beer-Lambert's Law in Pulse Oximetry [6]

2.2.4 Saturation versus Normalized Ratio

Normalization is needed for the measured light intensities at the different wavelengths because LEDs can emit light with different intensities. In addition, since LEDs are not monochromotic, their intensity propagates over a spectrum of wavelengths. According to the difference of wavelengths, the absorbing characteristics of the DC components and the sensitivity of the photo detector differ. Optical path length and tissue absorption also differ from patient to patient and the place of the probe [43]. The normalized signal I_n is determined by dividing the transmitted light intensities to their maximum peaks ($I_{\mathrm{H,R}}$ for the red wavelength and $I_{\mathrm{H,IR}}$ for the infrared wavelength). From Equation 2.11, it is derived as;

$$I_n = \frac{I}{I_H} = e^{-[\varepsilon_{Hb}(\lambda)c_{Hb}+\varepsilon_{HbO_2}(\lambda)c_{HbO_2}]\Delta d} \qquad 2.12$$

The intensity of the normalized signals $I_{\mathrm{H,n}}$ are independent of incident light levels and photodetector nonlinearities as shown in Figure 7.

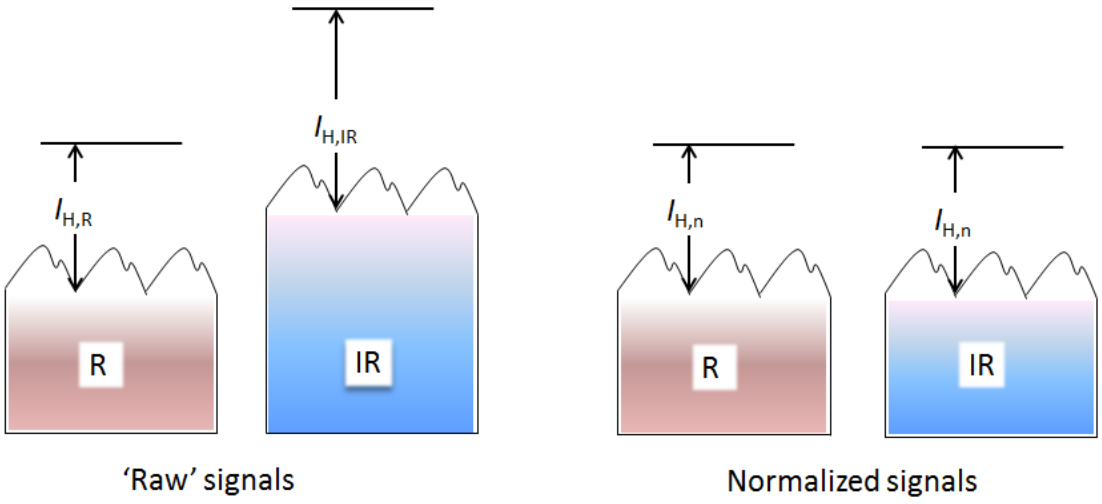

Figure 7 Raw and normalized signals [6]

The aim is to mention total absorbance with only AC components in the pathway, and it can be achieved by dividing the raw signal by the transmitted light in diastole as in Equation 2.13. The new constant incident light can be represented by the transmitted light during diastole and the ratio (R) of normalized absorbance at the red and infrared wavelengths depends only on the light absorbers present in the arterial blood.

$$R = \frac{A_{t,R}}{A_{t,IR}} = \frac{ln\left(I_{L,R}/I_{H,R}\right)}{ln\left(I_{L,IR}/I_{H,IR}\right)} \tag{2.13}$$

By using Equation 2.12, R can be derived as;

$$R = \frac{\left[\varepsilon_{Hb}(\lambda_R)c_{Hb} + \varepsilon_{HbO_2}(\lambda_R)c_{HbO_2}\right]\Delta d_R}{\left[\varepsilon_{Hb}(\lambda_{IR})c_{Hb} + \varepsilon_{HbO_2}(\lambda_{IR})c_{HbO_2}\right]\Delta d_{IR}} \tag{2.14}$$

If the optical path length for both red and infrared light is equal, only the arteries change their diameter. By using Equation 2.8 R can be expressed as;

$$R = \frac{\varepsilon_{Hb}(\lambda_R) + \left[\varepsilon_{HbO_2}(\lambda_R) - \varepsilon_{Hb}(\lambda_R)\right]SaO_2}{\varepsilon_{Hb}(\lambda_{IR}) + \left[\varepsilon_{HbO_2}(\lambda_{IR}) - \varepsilon_{Hb}(\lambda_{IR})\right]SaO_2} \tag{2.15}$$

The form of the ratio R shown in Equation 2.15 is independent from the optical path length and can be derived from the arterial oxygen saturation instead of the concentration of the hemoglobins in the blood [43].

2.2.5 Validity of Beer-Lambert's Law in Pulse Oximetry

SaO_2 can be expressed as a function of the measured and calculated ratio R with rewriting the Equation 2.15 as;

$$S_aO_2 = \frac{\varepsilon_{Hb}(\lambda_R) - \varepsilon_{Hb}(\lambda_{IR})R}{\varepsilon_{Hb}(\lambda_R) - \varepsilon_{HbO_2}(\lambda_R) + [\varepsilon_{HbO_2}(\lambda_{IR}) - \varepsilon_{Hb}(\lambda_{IR})]R} \times 100\% \qquad 2.16$$

It is shown that, the ratio R of measured and normalized total light arbsorbances in red and infrared can be calculated theoretically. Using extinction coefficients and R value theoretical oxygen saturation by Beer-Lambert's law can be calculated. But Beer-Lambert's law only considers the absorbed and transmitted light. In fact there is also reflected or scattered light while the incident light passing through the tissue [6]. Therefore, pulse oximeter should be calibrated based on empirical studies in healthy human volunteers to have a linear relation between R and SpO_2. The theoretical versus emprical calibration curve is shown in Figure 8.

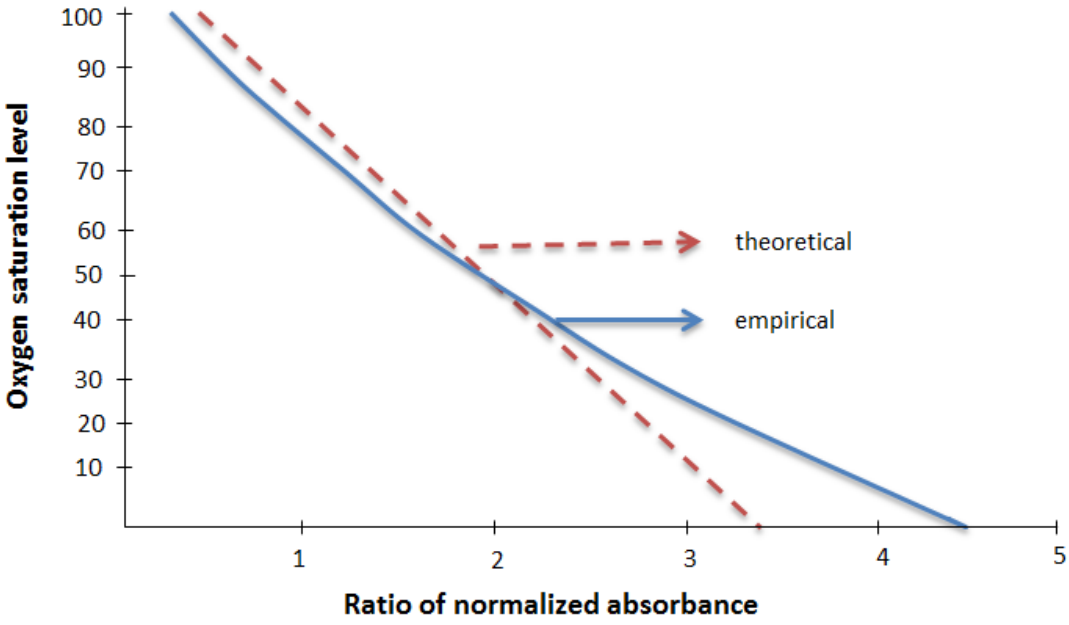

Figure 8 Theoretical versus empirical calibration curves [6]

According to the empirical studies relation between R and SpO_2 can be expressed as;

$$SpO_2 = a - b \times R \quad 2.17$$

a and *b* are coefficients that are determined from simple linear regression analysis when the pulse oximeter is being calibrated.

2.2.6 Types of Pulse Oximetry

There are two types of pulse oximeters which are reflective and transmission. Both reflective and transmission type pulse oximeters use the same technology but differ in positioning the sensors. As the name implies, the reflected light is measured by using the reflective pulse oximeter and the transmitted light is measured by using the transmission pulse oximeter. LEDs and photodiode are placed reciprocally in the probe in the transmission pulse oximeters as shown in Figure 9.

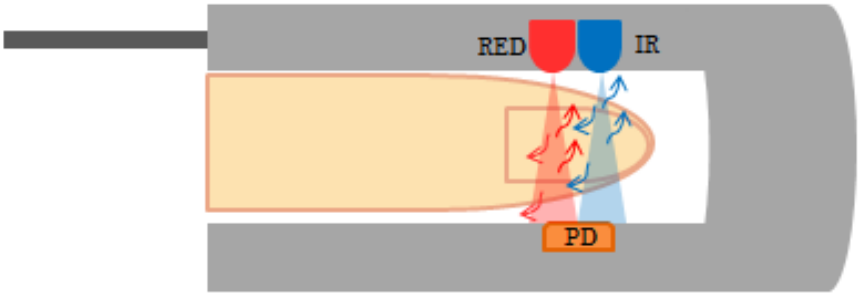

Figure 9 LEDs and photodiode position in the transmission pulse oximeter

Transmission types of pulse oximeters are used on limited areas of the body such as finger and ear tip. Because LEDs and photodiode should be placed in close proximity to obtain transmitted light effectively. Since reflective type pulse oximeters does not require reciprocal placement of the receiver and the transmitter, the field of usage in the body is broader such as chest, abdominal or forehead.

2.3 Thermocouple Working Principle

All materials are made up of electrons and these electrons are activated when the conductive materials are heated. The activation differs according to the conductor type. Using this difference between the conductors, thermocouples are made by using two dissimilar metals, joined together at one end.

Peltier effect states that if two different metals are connected together, a small voltage called a thermo-junction voltage occurs at the junction. Besides, Thompson effect implies that if the temperature of the junction changes, voltage between the junction and the free ends would also change [44]. Combining these two effects produce Seebeck effect which points out that the temperature at the sensing junction can be determined by holding one junction at a known temperature (reference junction). The schematic drawing of a thermocouple is shown in Figure 10.

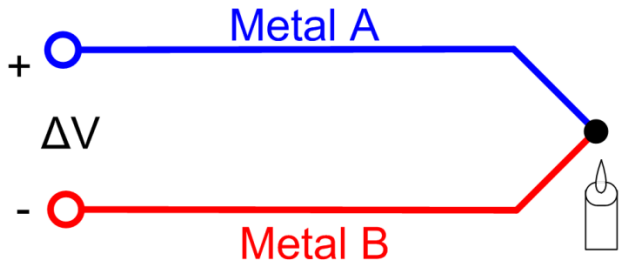

Figure 10 Schematic drawing of a thermocouple

The open circuit voltage ΔV directly proportional to the temperature change as calculated with Equation 2.18 [45].

$$\Delta V = \alpha_s \times \Delta T \qquad 2.18$$

In Equation 2.18, α_s is the Seebeck coefficient expressed in µV/°C, ΔT is the temperature change and ΔV is the voltage change.

To measure different temperature ranges, combination of different metals is used. Therefore, there can be infinite number of thermocouple combinations, but the Instrument Society of America (ISA) recognizes 12 of them [44]. The list of commonly used thermocouple types are shown in Table 2.

Table 2 Commonly used thermocouple types

Type	Positive Material	Negative Material	Range °C
B	Pt, 30%Rh	Pt, 6%Rh	50 to 1820
C	W, 5%Re	W, 26%Re	0 to 2315
D	W, 3%Re	W,25%Re	0 to 2315
E	N, 10%Cr	Cu, 45%Ni	-270 to 1000
G	W	W, 26%Re	0 to 2315
J	Fe	Cu, 45%Ni	-210 to 1200
K	N, 10%Cr	Ni,2%Al,2%Mn,1%Si	-270 to 1372
N	Ni, 14%Cr,1.5%Si	N, 4.5%Si,0.1%Mg	-270 to 1300
R	Pt, 13%Rh	Pt	-50 to 1768
S	Pt, 10%Rh	Pt	-50 to 1768
T	Cu	Cu, 45%Ni	-270 to 400

The most frequently used thermocouple type in sleep testing is type E or type T [46]. Type T uses copper-constantan wires with a sensitivity of approximately 43μV/°C [46] . Electrical connection of the different wires in the oronasal thermocouple is shown in Figure 11 [46]. Nasal sensors are the two reactive beads going up and the oral sensor is the one going down.

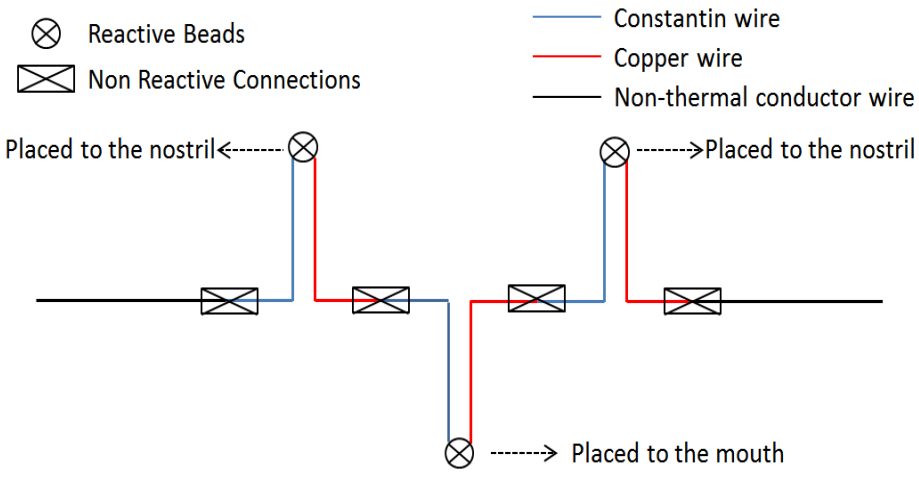

Figure 11 Thermocouple sensor wiring diagram

The advantages of thermocouples are the immunity to shock and vibration, ability to use over a wide temperature range and simple to manufacture. In addition, they do not need excitation power, do not have problem about self-heating and can be made very small. On the opposite side, the output of the thermocouples is very low and requires a sensitive and stable measurement.

CHAPTER 3

DESIGN OF SLEEP APNEA DETECTION AND MONITORING SYSTEM

3.1 Introduction

Portable sleep apnea detection system is comprised of five main parts. These parts are sensors, analog hardware, Bluetooth communication, ARM based software design and mobile application. Sensors are the source of the temperature and PPG data. Analog hardware is the analog readout circuit which includes amplifiers and filters, and it is used to receive analog signal from sensors. ARM based software consists of sleep apnea detection, heart rate and SpO_2 calculation algorithms. Mobile application is used for monitoring and recording the requested data. Data transfer between ARM processor and the mobile application is established on Bluetooth communication. Design and implementation of these parts of portable sleep apnea detection and monitoring system is explained in this chapter briefly. Block diagram of the entire system is shown in Figure 12.

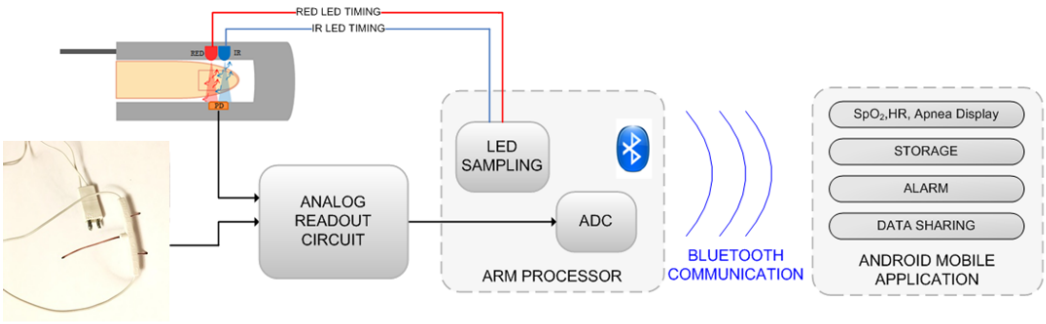

Figure 12 Block diagram of the entire system

3.2 Sleep Apnea Detection and Monitoring Design Requirements and System Specifications

- In biomedical systems, the most important requirement is satisfying the electrical safety. In case of any leakage current, high amount of current may occur from the power line and may be passed through conductive probes to the patient body. In this system, pulse oximeter and thermocouple probes are used and they are physically attached to the patient body. The pulse oximeter probe is an isolator itself; it contains LEDs and a photodiode. Secondly, thermocouple probe does not need an excited power; it produces its own voltage at the output junction. In addition, the system works by 3V battery and there is not any connection to power lines. Therefore, there is no risk for leakage current.
- As stated in chapter 2.3, the output voltages of the thermocouple and the photodiode are in the order of microvolts. Therefore, there is a need for high gain amplification to provide proper signal for data acquisition system. The analog design of the sleep apnea detection system includes two instrumentation amplifiers to set gain at 5000 for the thermocouple output and one dual operational amplifier to set gain at approximately 3000 for the photodiode output. By arranging these gain values, amplified signals are kept in ADC input voltage range (0-5V).
- Because of the fact that low amplitude level of the sensor output signals, robustness to environmental electrical noise is very important, especially for thermocouple output. To obtain good noise cancellation capability, instrumentation amplifier is used to remove common mode noise from the thermocouple output signal. In this sense, CMRR of the thermocouple readout system is measured 124 dB at 1 Hz. In addition, using analog RC filters, unwanted DC signal, and high frequency noise are removed from the respiration and pulse oximeter signal in the analog readout circuitry. For the respiration signals higher frequencies from 1.06Hz and for the pulse oximeter signals out of frequency band 0.6-3.2 Hz are suppressed.

- Resolution of ADC is important to decrease quantization error during conversion. AtMega368 ARM processor is used in this system, and it has 10-bit ADC inside. Taking into account the size of data transfer between sleep apnea detection module and an Android device, 10-bit resolution is considered sufficient.
- Data acquisition speed between analog circuitry and ARM processor should be considered. According to the Nyquist sampling theorem, sampling rate for the thermocouple output signal is arranged as 100 Hz and sampling rate for pulse oximeter signal output is arranged as 50 Hz.
- In portable systems, power consumption is very remarkable point. Sleep apnea detection and monitoring system has 80mA current consumption. Therefore, it is designed to operate with two 1.5V Li-Ion battery with 2400mA/h current capacity. This means; the battery can be used in full performance for 30 hours.
- Due to the fact that, sleep apnea detection and monitoring system is used during sleep, it should be low weight, may be wearable and comfortable. For this reason, Android devices are used for monitoring to avoid LCDs, thus reducing power consumption, weight and size. Communication between mobile phone and the system is established on Bluetooth to eliminate cabling. The system overall weight is approximately 105 gr.

3.3 Sensors used in this Study

3.3.1 Thermocouple

Salter Labs 5800T thermocouple is used to obtain oral and nasal respiration data. Thermocouple probe is shown in Figure 13.

Figure 13 Salter Labs 5800T disposable thermocouple

Owing to the fact that larger temperature changes produce larger signal amplitude, positioning the oronasal thermocouple in close proximity to the nostrils and mouth is important. Thermocouple temperature response is analysed to see the maximum and the minimum voltage output regards to the input temperature. Output is the thermocouple readout circuit output which means after low pass filter and amplification with 5000 gain.

Thermocouple probe is placed inside a temperature cabin and temperature is increased from 15.5°C to 40°C. After that without opening the cabin door, temperature of the cabin is decreased from 40°C to 15.5°C. Temperature cabin is reached to 15.5°C from 40°C at 5 minutes. During the temperature decrease, cabin temperature value is recorded at 5 seconds intervals. Measured temperature response of the thermocouple while the cabin temperature is decreasing from 40°C to 15.5°C is shown in Figure 14.

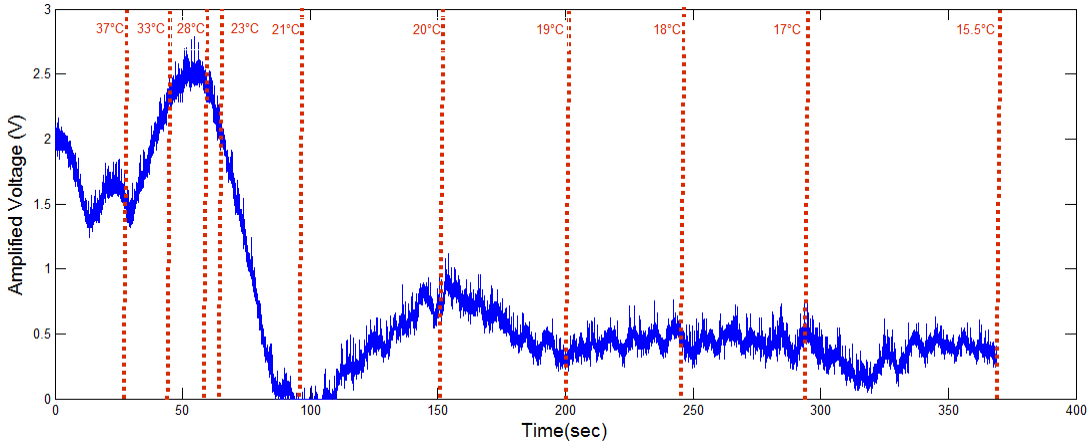

Figure 14 Measured thermocouple temperature response (40°C - 15.5°C)

3.3.2 Pulse Oximeter Probe

Nellcor disposable finger type pulse oximeter probe is used to obtain PPG data. In this transmission type pulse oximeter, one LED emits red light with a wavelength of 660 nm, the other LED emits infrared light with wavelength of 940 nm and the photodetector has a peak sensitivity of 850 nm. Pulse oximeter probe is shown in Figure 15.

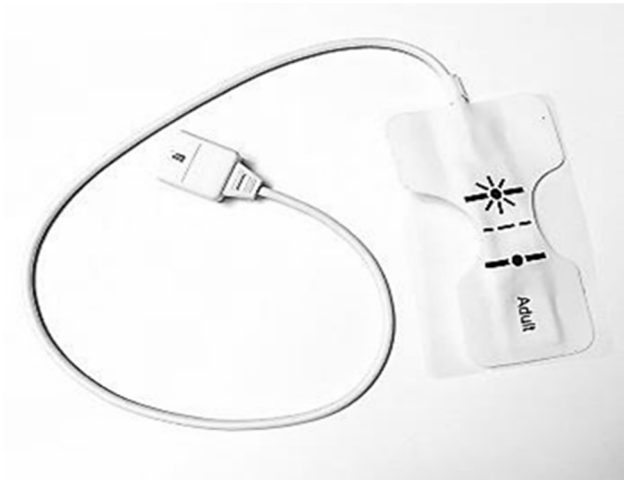

Figure 15 Nellcor disposable pulse oximeter probe

Pulse oximeter probe has infrared and red LEDs as transmitter and one photodiode as receiver. The LEDs are connected end to end and excited sequentially by ARM processor (ATmega328P).

3.4 Analog Hardware

Analog hardware of sleep apnea detection and monitoring system is composed of three parts. The first part is the power circuit for voltage conversion and regulation, the second part is thermocouple readout circuit for filtering and amplifying the low amplitude thermocouple sensor output and the final part is pulse oximeter readout circuit for filtering and amplifying the photodiode output.

3.4.1 Power Circuit

Power circuit is responsible to supply required electrical power to the analog circuit, ARM processor and Bluetooth device. As stated in the system requirements part, the system should be portable, low profile and has minimal power consumption. Therefore, the system is designed to work with only 3V by using 2xAAA Li-Ion battery. Block diagram of the power circuit is shown in Figure 16.

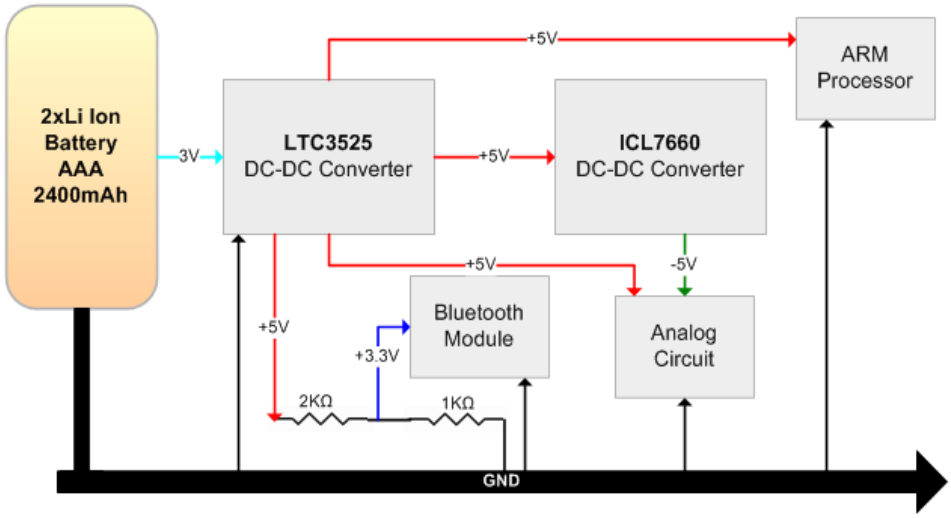

Figure 16 Power circuit block diagram

Li-Ion battery is chosen due to its low size, high current capacity, and easy to achieve. Overall power consumption of the system is approximately 80mA. Therefore, with current capacity of 2400mA/h battery, the sleep apnea detection system can be operated for 30 hours. The maximum current capacity of coin cell or button cell batteries is 600mAh and this provides current to the sleep apnea detection system only for 7.5 hours.

LTC3525 is used to convert the received 3V battery voltage to +5V with an approximately output current of 300mA. LTC3525 is a compact and high efficiency solution for charge pumps in a dual cell Li-Ion application. After the start up, it can maintain regulation with a low input voltage of 0.5V. In addition, it requires only three small external components to operate. 5V is used to feed the ARM processor, the analog circuit and the Bluetooth unit over a voltage divider. 5V is also the input of ICL7660 CMOS voltage converter which is used to convert +5V to -5V to supply required negative bias voltage to the instrumentation amplifiers in the thermocouple analog readout circuit. ICL7660 is also a small and efficient solution for a negative voltage converter that has a voltage converter efficiency of 99.9% and a power efficiency of 98%. Moreover, it needs only 2 polarized electrolytic capacitors as an external component.

3.4.2 Thermocouple Readout Circuit

The output voltage of the thermocouple sensor mentioned in 3.3.1 is approximately 200μVpp at 22°C which is very low. Therefore, the output of the thermocouple should be amplified to obtain respiration signal without noise. Instrumentation amplifiers (IA) are mostly used in medical applications, since they have relatively higher common mode rejection ratio (CMRR) than the operational amplifiers [47]. High CMRR provides less change in common mode voltage at the output. Instrumentation amplifier is a type of differential amplifier. Although it is not achievable in practice, it is desired that an ideal differential amplifier would have

infinite CMRR. If this were the case, an equally applied signal to the both inputs of an op amp would have no effect at the output. IAs are composed of three-amplifier design [48]. The first and the second amplifiers are used for buffering and reducing the common mode signal. Buffering creates high input impedance for the amplifier and it is an important advantage for thermocouple circuits so that the thermocouple output voltage is too low. The last amplifier is used as a difference amplifier to amplify the difference between the input signals.

While implementing the instrumentation amplifier design, the major problem is the requirement to use very close matching resistors in order to keep the gains same. A little mismatch between the two inputs will cause a considerable effect on performance and a degradation of CMRR. Therefore, commercial integrated IAs are available on a single package IC. AD620 of Analog Devices company is used as an instrumentation amplifier in the thermocouple readout circuit. AD620 provides an opportunity to set gain by using only one resistor and no auxiliary elements are needed for operation.

Block diagram of the thermocouple readout circuit is shown in Figure 17.

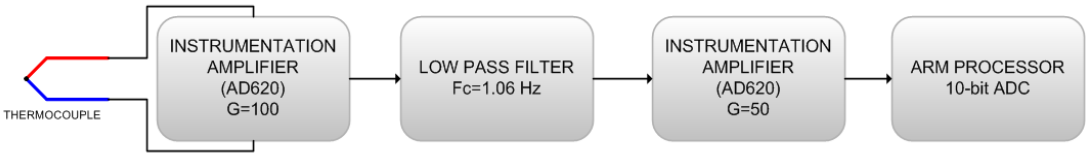

Figure 17 Thermocouple readout circuit block diagram

Passive low pass filter is used after the amplification of the analog signal to avoid undesired high frequency components of mains and PCB circuit. The magnitude and phase responses of the low pass filter with a cut of 1.06Hz is shown in Figure 18.

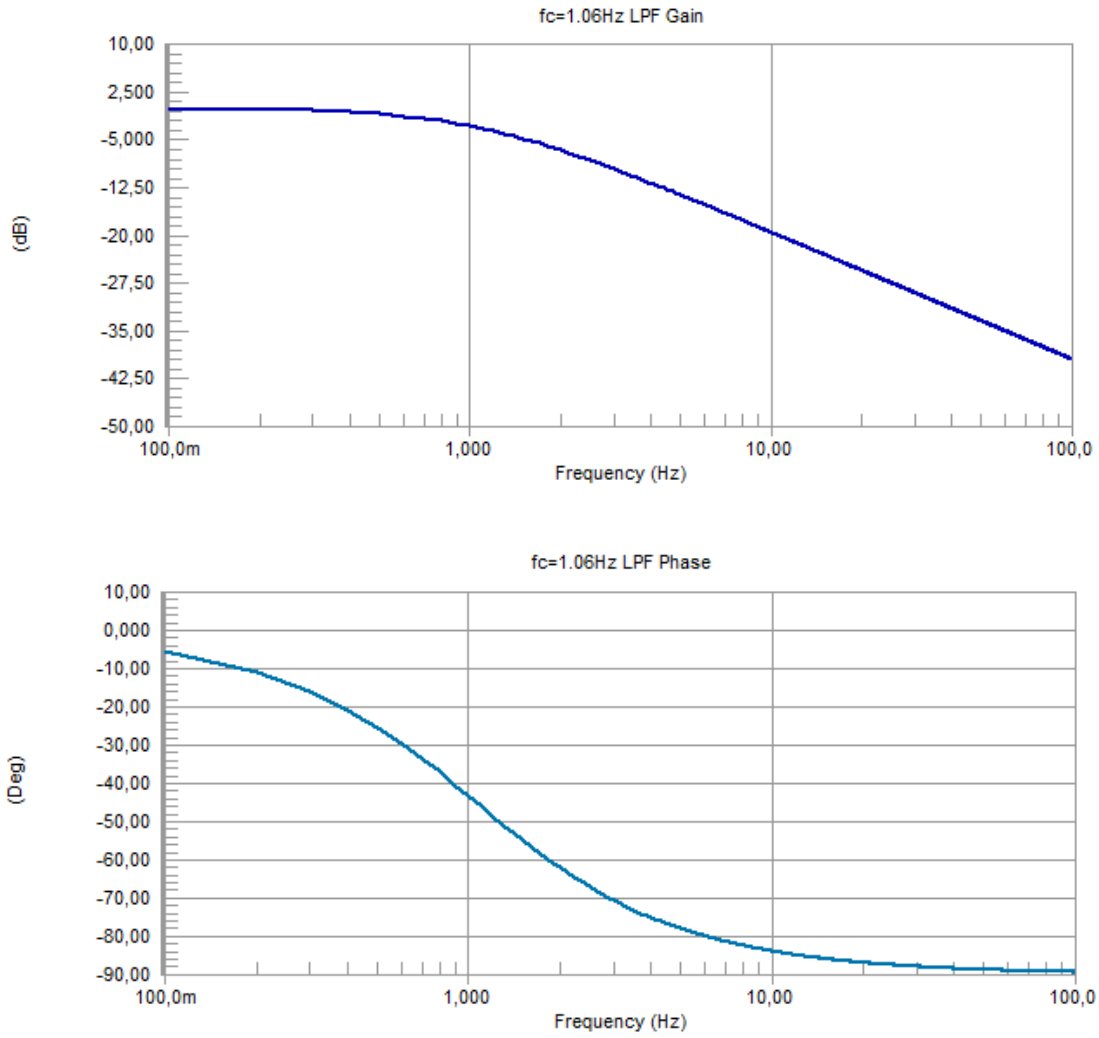

Figure 18 Magnitude and phase response of the low pass filter used in thermocouple analog readout circuit (f_c=1.06 Hz)

3.4.3 Pulse Oximeter Readout Circuit

As stated in 3.3.2, because of the sequentially excited LEDs, current occurs as an output of a photodiode. PPG signal occurring at the output of the photodiode is low amplitude, noisy, and has DC component. Therefore it should be filtered and amplified. Passive high pass filter with ~0.6Hz cut-off frequency is used to block the DC component and low pass filter with ~3.2Hz cut-off frequency is used to eliminate

high frequency noise. Block diagram of the pulse oximeter readout circuit is shown in Figure 19.

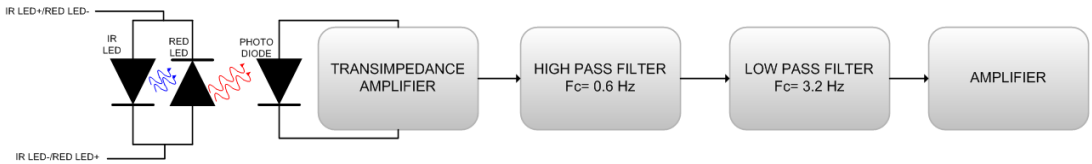

Figure 19 Pulse oximeter readout circuit block diagram

Magnitude and phase responses of the low pass filter with a cut of 3.2 Hz is shown in Figure 20.

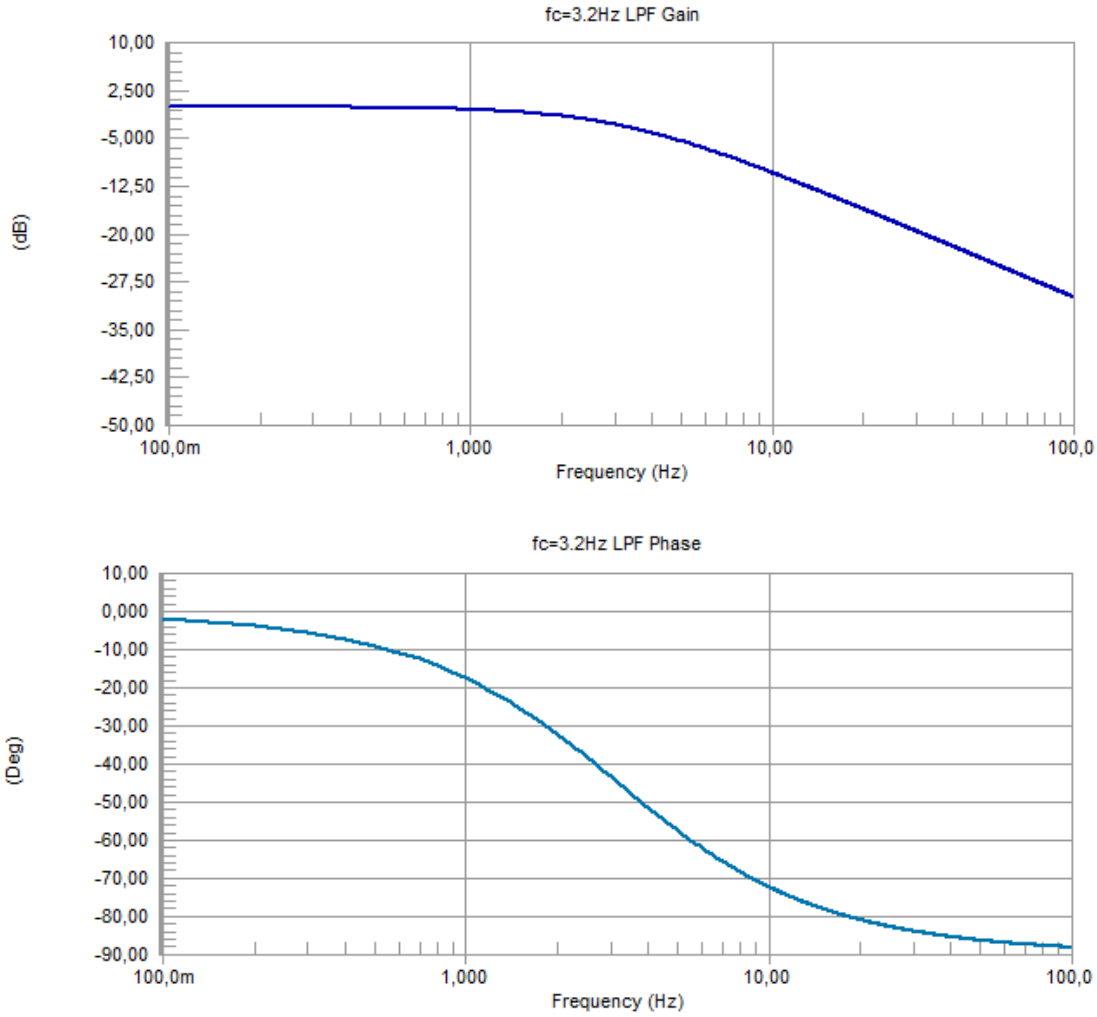

Figure 20 Magnitude and phase response of low pass filter used in pulse oximeter analog readout circuit (f_c=3.2 Hz)

Magnitude and phase responses of the high pass filter with a cut of 0.6 Hz is shown in Figure 21.

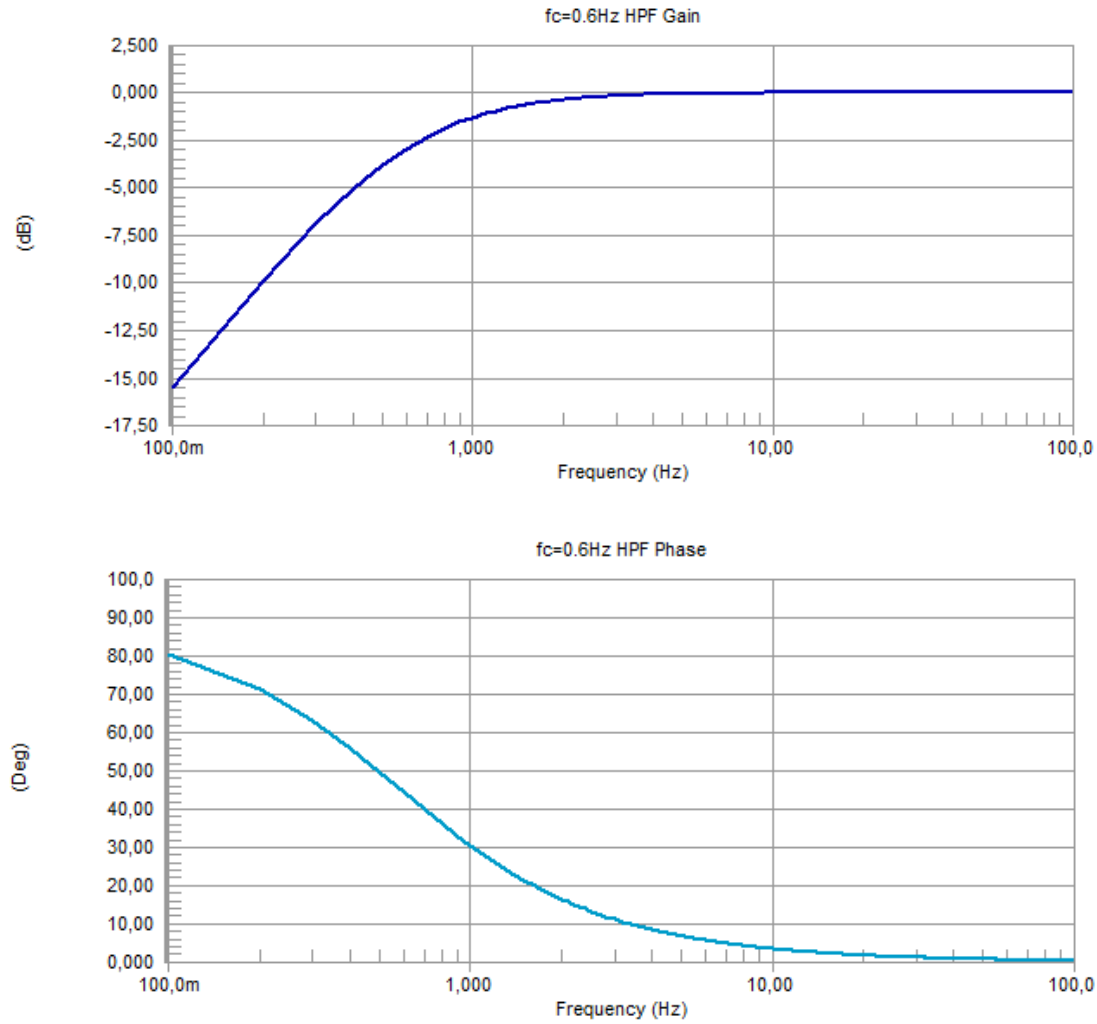

Figure 21 Magnitude and phase response of low pass filter used in pulse oximeter analog readout circuit (f_c=0.6 Hz)

Two stage operational amplifier is used to obtain high gain. LM358-N is chosen as an operational amplifier, because it has wide power supply range and suitable for both single and dual supply. It has two internally compensated operational amplifiers which help to minimize the size of sleep apnea detection system. In the first stage, filtered photodiode output is amplified 150 times and in the second stage signal is amplified 22 times. As a result, the total gain is obtained approximately 70dB.

3.5 Bluetooth Communication

Bluetooth communication is based on IEEE 802.15.1 Wireless Personal Area Network standard [49]. Bluetooth is like the RF version of serial communication and is used for short range, low power consumption applications of portable devices. The industrial, scientific and medical (ISM) radio band is used to operate Bluetooth protocol at 2.4Gz. Cordless phones, near field communication (NFC) devices and wireless computer networks (WiFi) also use ISM radio band. There is a need for external antenna for WiFi modules, and this consumes too much space for the portable device. NFC devices are limited of communication distance that they should be close to the communicated device with 4 cm. Because of the drawbacks of Wifi and NFC, using Bluetooth communication for wireless data transfer between mobile application and the ARM processor is inevitable for this study. HC-05 Bluetooth module is used to establish Bluetooth communication between ATmega358P and Android mobile device.

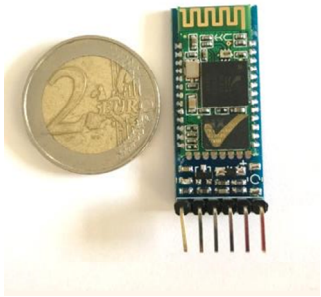

Figure 22 HC-05 Bluetooth module

Operating voltage of HC-05 is 3.3V. Therefore, ATmega358P 3.3V, GND, RX and TX pins are connected to VCC, GND, TX ans RX pins in the HC-05 module, respectively. HC-05 has user defined baud rates from 4800 to 1382400. But because of enough size of the parameters which are sent via Bluetooth, maximum baud rate is arranged as 115200 between Android and ARM processor. Technical specifications of the Bluetooth module are shown in Table 3.

Table 3 Technical specifications of HC-05 Bluetooth module

Bluetooth Protocol	Bluetooth Specification v2.0
Size	1.1 x 0.5 x 0.1 inches
Modulation	GFSK (Gaussian Frequency Shift Keying)
Baud Rate	115200 (user defined baud rate) (4800 to 1382400)
Range	Class 2 (~10m)
Voltage	3.3V (2.7V – 4.2V)
Speed	Synchronous 1 Mbps
	Asynchronous 2.1 Mbps

Master/Slave model is used in Bluetooth networks to control the data transportation between devices. HC-05 Bluetooth module can be set to be either Master or Slave. The master coordinates communication which can send data to any of slaves and request data from them. But slaves can only transmit to and receive from master. In the sleep apnea detection system, HC-05 Bluetooth module is slave which transmits data to the android device.

3.6 Mobile Application

Mobile application is developed for displaying, recording and sharing the required data. Since the data communication is based on Bluetooth and the Android operating system is convenient to use with Bluetooth APIs, Android is chosen as the operating system. Application is developed with MIT App Inventor which is a tool to transform complex language of text-based coding into visual, drag and drop building blocks. In the mobile application; after the Bluetooth link is up, heart rate, SpO_2 and number of sleep apnea data collected from the patient are displayed for the whole sleep cycle. Apnea index is calculated when the record is stopped by dividing number of total apnea events to total sleep hour. With share record button, whole sleep record can be shared via e-mail or other social accounts to the doctors or to the

related people. If there is a case where the cessation takes longer than 30 seconds during the sleep, alarm is rung to wake up the patient or the bed partner to avoid the fatal risks. Visualization of the mobile application is shown in Figure 23. MIT App inventor blocks may be found in APPENDIX A.

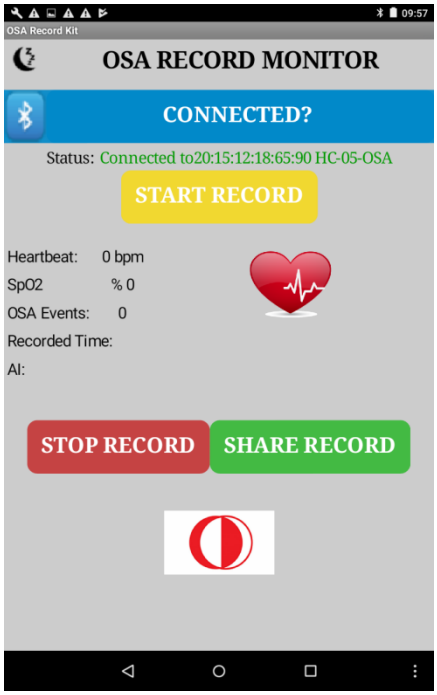

Figure 23 User interface of Android mobile application

3.7 ARM Software Design

System software is comprised of two parallel algorithms. First algorithm is used to detect sleep apnea from respiration and the second one is used to calculate SpO_2 and heart rate. Results of these algorithms are evaluated separately. SpO_2 and heart rate information of the whole night sleep is recorded in mobile device through Bluetooth communication to be able to share data with e-mail. In other words, SpO_2 and heart rate information is not used to detect apneic attack, these signals are used to give additional information to the clinicians. Only respiration signal which is obtained from a thermocouple is used to detect apnea and activate the alarm of the mobile device to wake up the patient when the apneic attack takes longer than 30 seconds.

3.7.1 Algorithm of Sleep Apnea Detection from Respiration

A typical airflow sensor data which is detected by an oronasal thermocouple and obtained from Physionet SHHS (Sleep Heart Health Study) database is shown in Figure 24.

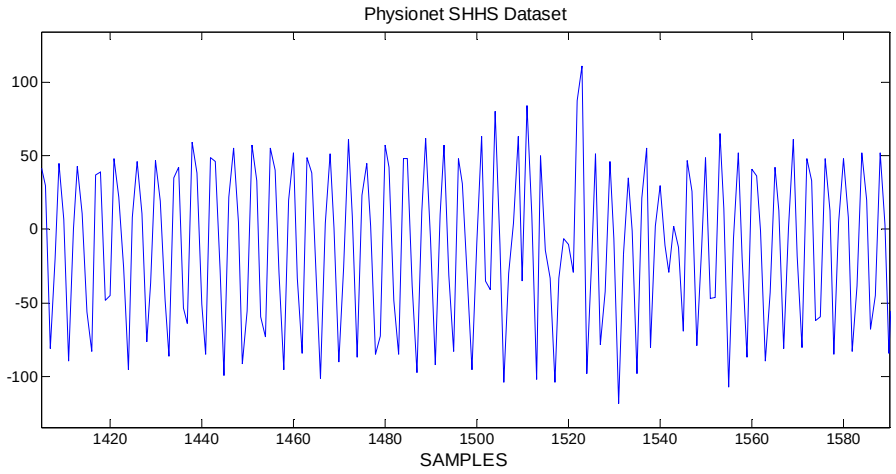

Figure 24 A segment of airflow signal with normal breathing obtained from Physionet SHHS database [50]

It can be seen that, there is a certain rhythm and the energy level in the normal respiration signal [33]. Apnea can be detected by correlating the absence of energy and a lack of rhythm. But motion artefacts or sensor noise also affects the energy level of the signal. Therefore by using threshold crossing method (based on zero crossing), normal breath and the sleep apnoeic attack can be distinguished in real time. Block diagram of the sleep apnea detection algorithm from respiration is shown in Figure 25.

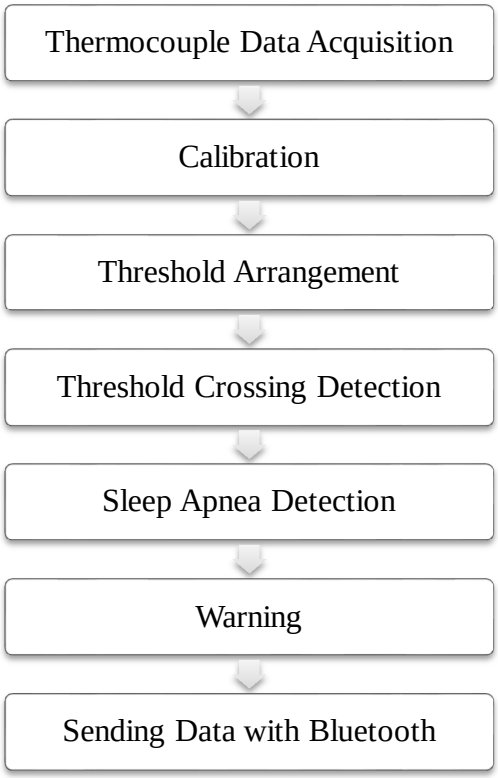

Figure 25 Sleep apnea detection from respiration algorithm block diagram

Thermocouple readout sampling frequency is arranged as 100 Hz. Because at rest, respiration frequency for adult and elderly people is not more than 0.5 Hz [51]. Frequency domain analysis shows the main frequency components of the respiration signal obtained through analog circuit from Subject-1 (description of the test database is stated in 5.3). In Figure 26, digitized signal y(t) of the respiration data from Subject-1 is shown, FFT of y(t) signal (Y(f)) is plotted in Figure 27 and the log magnitude of Y(f) is shown in Figure 28.

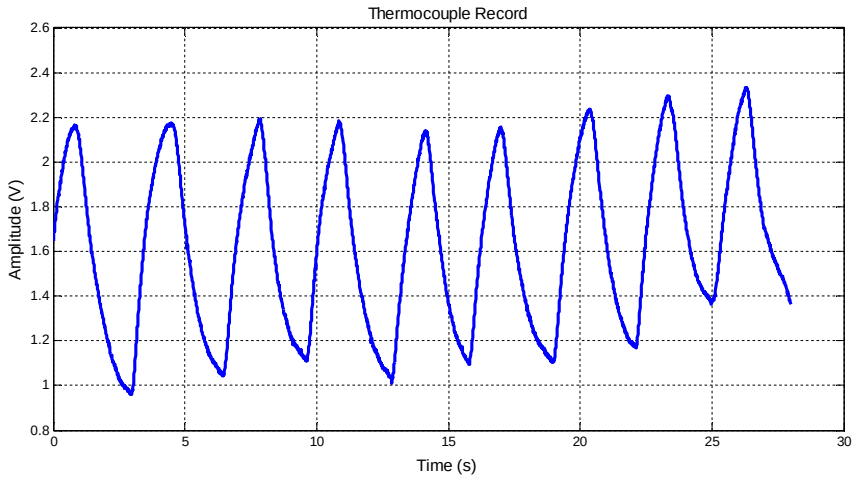

Figure 26 A part of a respiration signal of Subject-2, y(t)

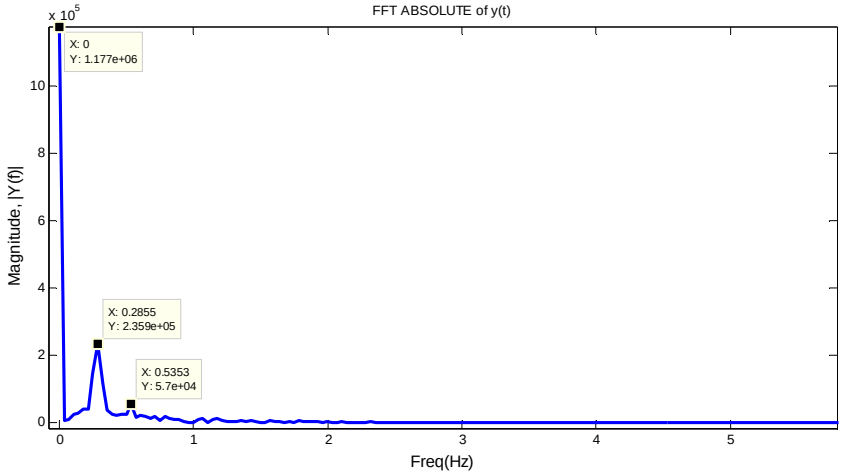

Figure 27 Zoomed in version of |Y(f)|

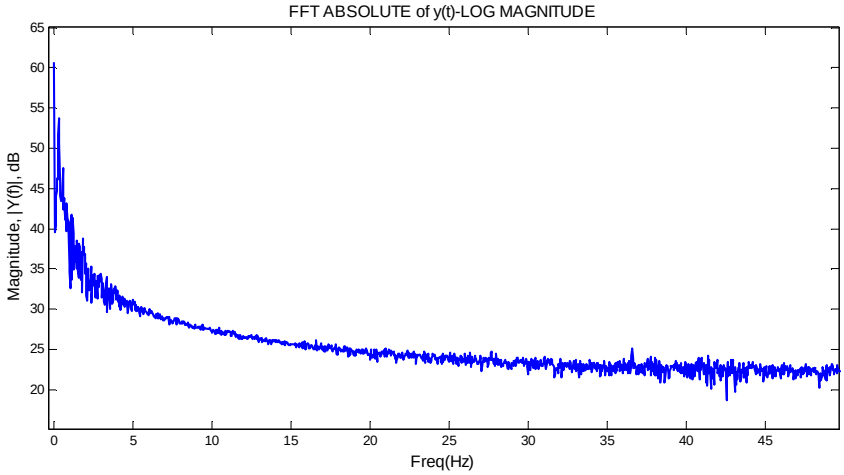

Figure 28 Log magnitude of |Y(f)|

As a result of respiratory effort, temperature change occurs in the nostrils. This temperature change generates voltage at output of the thermocouple. Zero crossing point detection algorithm is used to detect sleep apnea from respiration signal. Zero crossing is produced even if the consecutive two samples have different signs, therefore it can be calculated as multiplying these consecutive samples [52]. But the output of the thermocouple readout circuit is always positive because of the positive offset of hardware circuit. Therefore, there is a need to find threshold for the detection of crossing points. If *s(n)* and *s(n+1)* are the two consecutive points and Th_A is the amplitude threshold value for the respiration, threshold crossing points can be detected with the following formula:

$$s(n+1) \geq Th_A > s(n)$$
$$\text{or} \qquad (3.1)$$
$$s(n+1) \leq Th_A < s(n)$$

The visualization of threshold crossing point detection is shown in Figure 29.

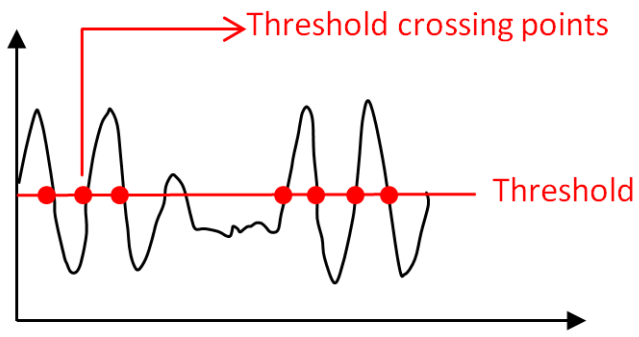

Figure 29 Visualization of threshold crossing point detection

Finding a generic value for the amplitude threshold of the thermocouple may not be applicable because amplitude of the thermocouple readout circuit output signal varies with the body temperature, respiration effort and position of the thermocouple in the nostrils. Using auto calibration which starts 40 seconds later the program begins and lasts 20 seconds is a solution to find amplitude threshold.

During the 20 seconds calibration duration, data is gathered at sampling frequency of 100 Hz and mean of this calibration data gives the amplitude threshold value to calculate threshold crossing points.

According to the maximum respiration frequency, time threshold is arranged as 2.5 seconds to eliminate false threshold crossing points [53].

3.7.2 Algorithm of SpO_2 and Heart Rate Calculation

Resulting from the pulsatile shape of the PPG signal, SpO_2 and heart rate calculation algorithm is based on the theory of finding maxima and minima named as the peak detection. This algorithm which is described in this study requires minimal storage and computation. In addition, there is no need for pre-processing, this makes the method suitable for real time applications. A three-point sliding window technique is used to identify PPG signal peaks [54]. A Signal illustrated in Figure 30 shows the signal with two local minimums and one local maximum.

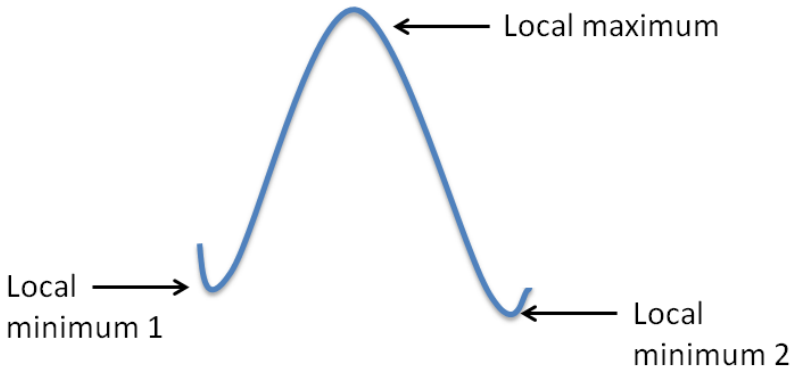

Figure 30 Local maxima and minima illustration of an arbitrary peak

If *x(i), i=1,2,…* represents the digitized signal with a sampling duration ΔT, the three-point sliding data window generates from *x(I+ -1)*, *x(I+)* and *x(I+ +1)*. At *i=I+*, the occurrence of the local maximum can be detected with the below term:

$$x(I^+ - 1) \leq x(I^+) > x(I^+ + 1)$$
$$\text{or} \qquad 3.2$$
$$x(I^+ - 1) < x(I^+) \geq x(I^+ + 1)$$

The term is arranged for the local minimum case *x(I⁻)* as;

$$x(I^- - 1) \geq x(I^-) < x(I^- + 1)$$
$$\text{or} \qquad 3.3$$
$$x(I^- - 1) > x(I^-) \leq x(I^- + 1)$$

In practice, three adjacent data points are not sufficient to find authentic peaks in the signal, because spurious peaks may occur due to artefacts and the saturation noise. Using threshold condition based on amplitude, duration or slope criterion or a combination of them is a solution to eliminate these spurious peaks [54]. Process sequence of heart rate and SpO_2 calculation algorithm is given in Figure 31.

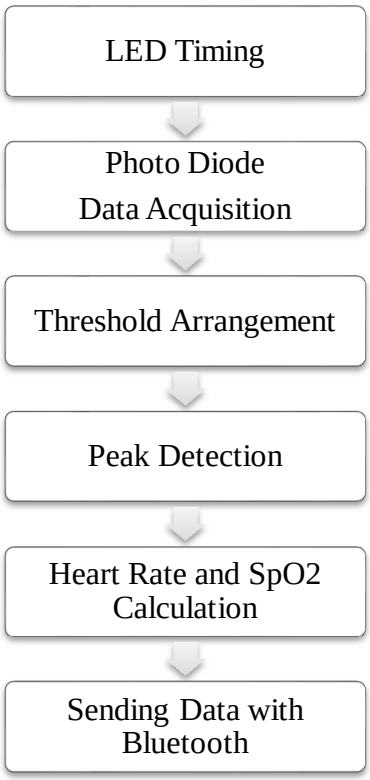

Figure 31 Process sequence of heart rate and SpO_2 calculation algorithm

As stated in 3.3.2, pulse oximeter probe has infrared and red LEDs as transmitter and one photodiode as receiver. The LEDs are connected end to end and are excited sequentially by ARM processor (ATmega328P). When the red LED is switched on, infrared LED is switched off and when the infrared LED is switched on, the red LED is switched off, which continues periodically until the end of the test. The switching of the two LED's is controlled with red and infrared timing digital signals at a sampling rate of 25 Hz. LED timing diagram is shown in Figure 32.

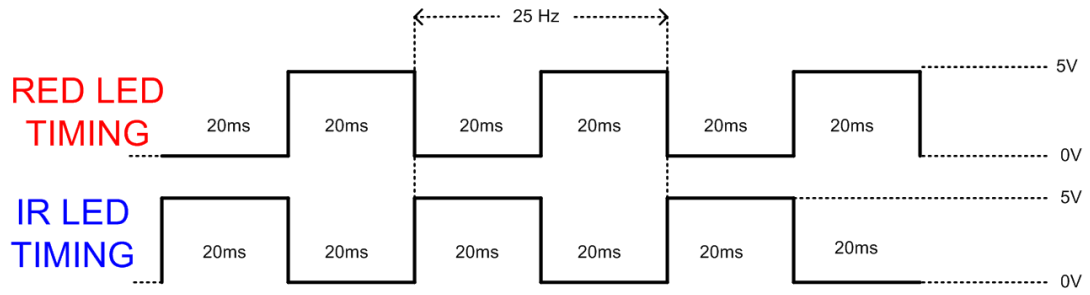

Figure 32 LED timing diagram

In the heart rate and SpO_2 calculation algorithm, LED blinking time composes of photo diode acquisition time. According to the red and infrared timing signals shown in Figure 32, LEDs are excited sequentially at a sampling rate of 25Hz. This means that photodiode sampling rate is 50Hz. Main frequency component of PPG signal is investigated in frequency domain and it is observed that the heart rate of adults at rest is approximately 1Hz. In Figure 34 and Figure 35, 0Hz component is the DC level of PPG signal, 0.99Hz component shows heart rate of Subject-1 and 25Hz component shows red and infrared LEDs timing frequency. A part of a PPG signal obtained from Subject-1 is also shown in Figure 33.

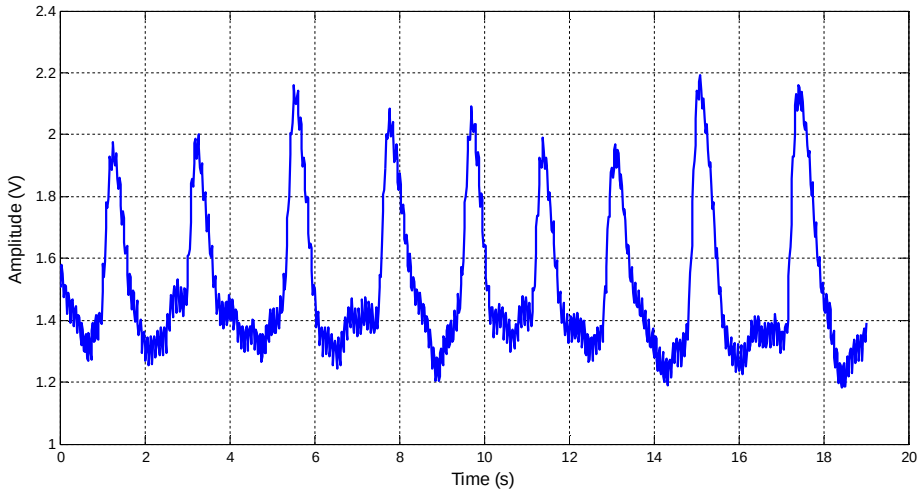

Figure 33 A part of a PPG signal of Subject-1, y(t)

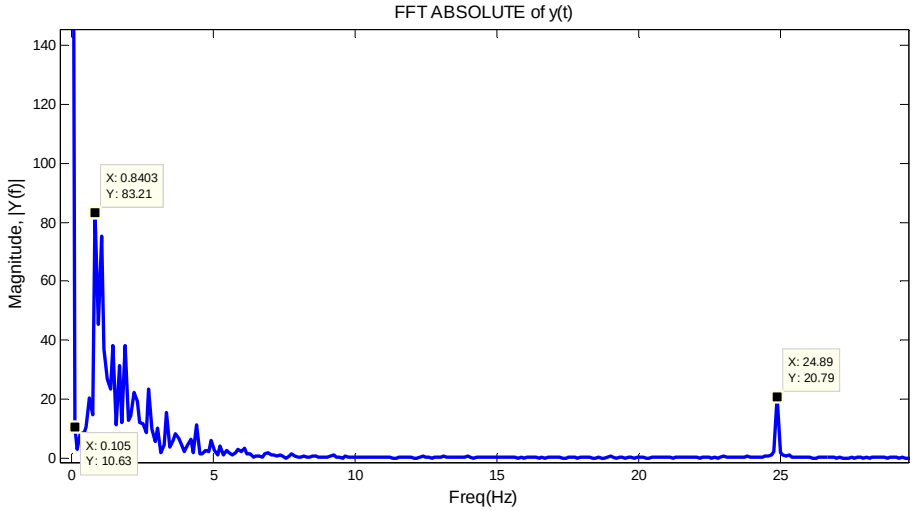

Figure 34 Zoomed in version of |Y(f)| (FFT of y(t) signal)

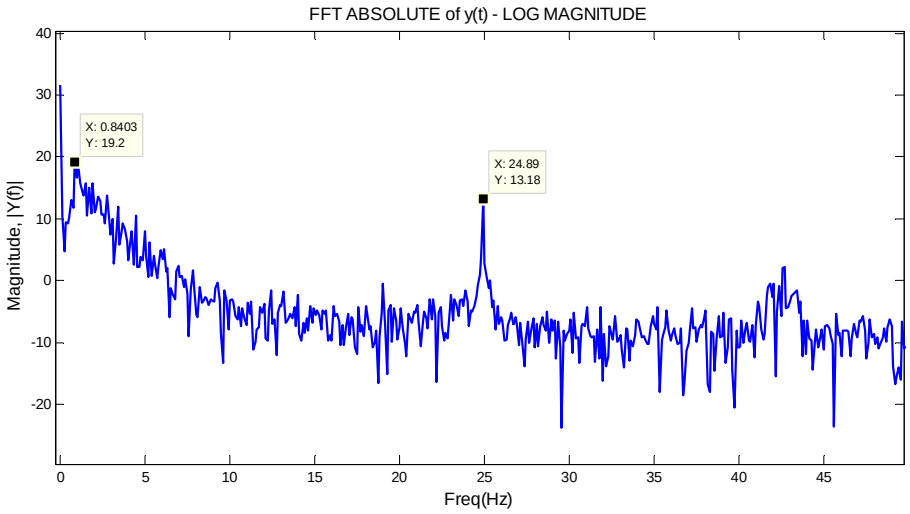

Figure 35 Log magnitude of |Y(f)|

Amplitude and time threshold should also be determined for real time SpO_2 and heart rate calculation. It is seen from the experiments that PPG signal amplitude does not change much between people. Therefore, amplitude threshold is arranged as the mean value of the amplified photodiode output as 1.5V. Time threshold is arranged according to the maximum heart rate of adults at rest. Since the maximum heart rate is accepted as 110bpm, time threshold for PPG signal is calculated as multiplying the maximum heart rate with 0.75 [55].

According to the technical guideline of American Association of Sleep Technologists (AAST) averaging time of calculating SpO_2 should be < 3 seconds [56]. Therefore, every 3 seconds SpO_2 is calculated and updated on the monitor. But heart rate is calculated each time a peak is detected. Flowchart of SpO_2 and heart rate calculation is given Figure 36.

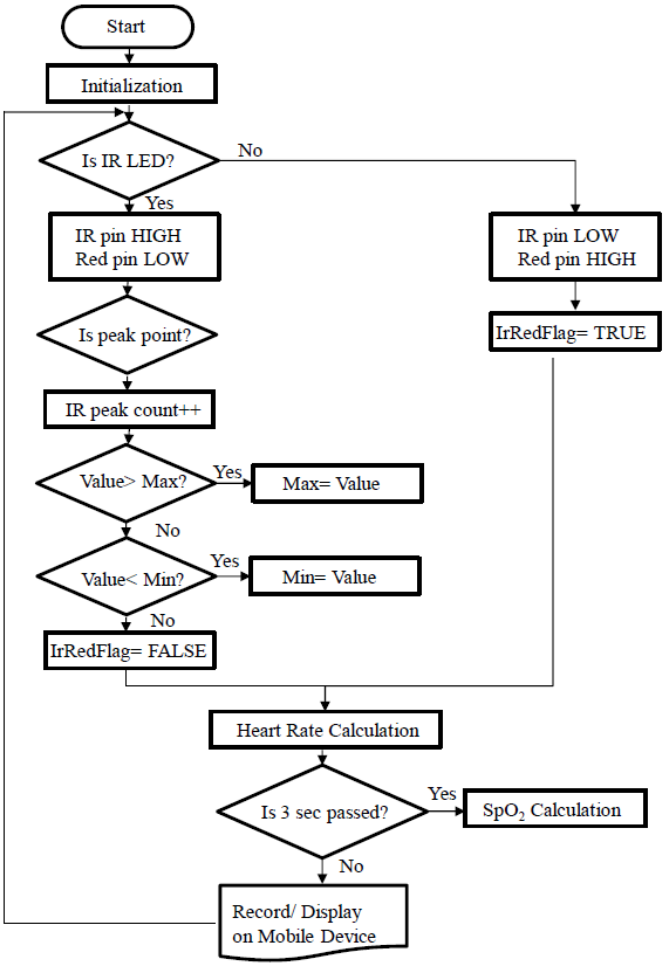

Figure 36 Flowchart of SpO_2 and heart rate measurement

CHAPTER 4

HARDWARE DESIGN and TEST MEASUREMENTS

4.1 Introduction

PCB and 3D prototyping outputs are shown in this chapter. Several tests to measure the performance of the portable sleep apnea detection system are performed and defined in this chapter.

4.2 Fabrication Outputs

Sleep apnea detection and monitoring system analog electronic circuit is designed in Altium Designer. In Figure 37, 3D visualization of sleep apnea detection system electronic cards and connectors is shown. Two layer PCB design of sleep apnea detection system after component placement and soldering is shown in Figure 38. Connector 1 is used for power input, connector 3 is for pulse oximetry sensor input, connector 5 is for thermocouple sensor input, and connector 4 is used for programming the AtMega368P ARM processor which is shown with number 2. The HC-05 Bluetooth module is numbered 6. To obtain the maximum efficiency from Bluetooth connection, the antenna part of the HC-05 is not closed with the PCB card. Final picture of the sleep apnea detection system with a box produced by a 3D printer is shown in Figure 39.

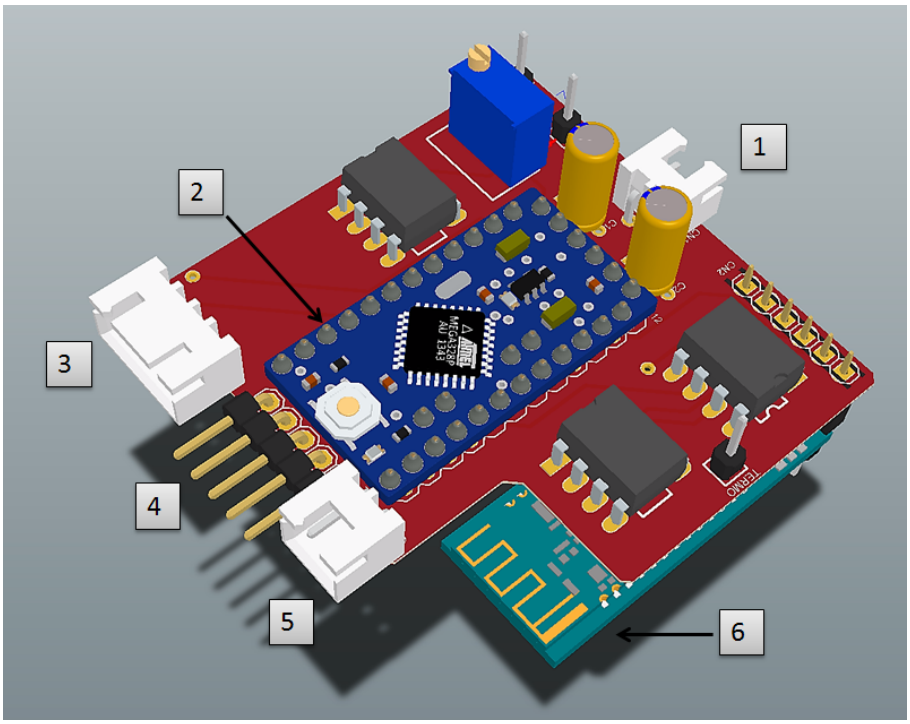

Figure 37 3D visualization of sleep apnea detection system electronic cards and connectors

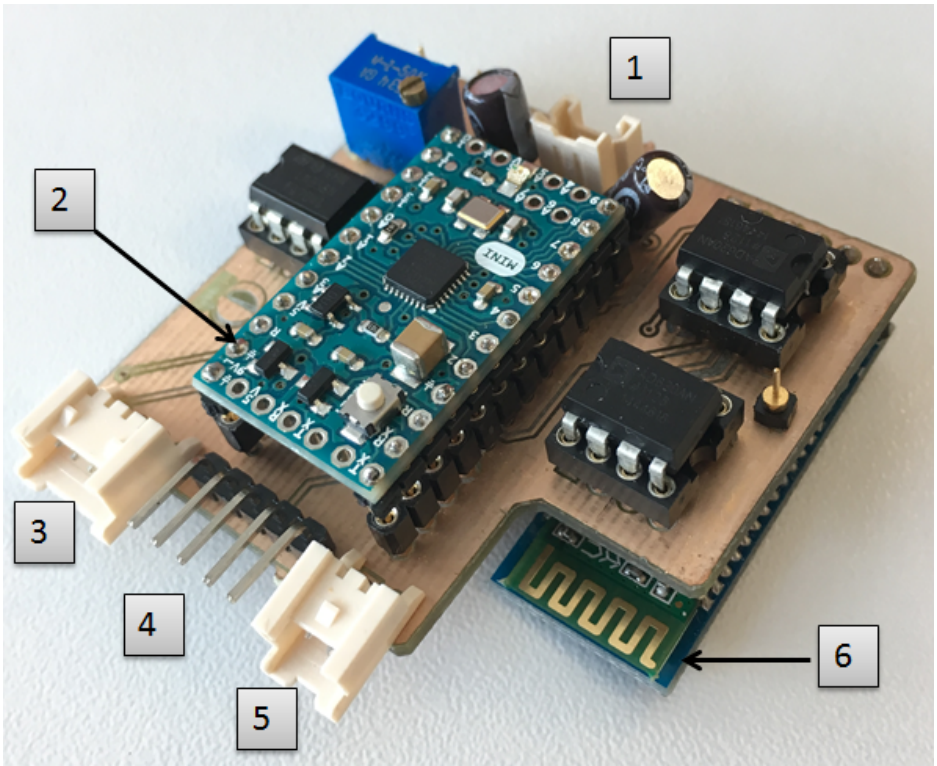

Figure 38 Two layer PCB design of sleep apnea detection system

Figure 39 Final picture of the sleep apnea detection system

4.3 Performance Tests of the System

4.3.1 Thermocouple Readout Circuit Tests

According to the low output voltage of thermocouple such as 200µVpp at 22°C, amplification without noise is important in thermocouple readout circuit. The gain equation of the used instrumentation amplifier (AD620) is given in Equation 4.1 where G states gain and R_G is the gain resistor.

$$G = \frac{49.4k\Omega}{R_G} + 1 \qquad 4.1$$

From to the gain equation thermocouple output is amplified approximately 100 and 50 times with R3 and R1 resistors in the first and second stage of the amplifier circuit, respectively. This makes the total gain 5000 and this corresponds to 74 dB gain.

$$G_1 = \frac{49.4k\Omega}{0.5k\Omega} + 1 \cong 100$$

$$G_2 = \frac{49.4k\Omega}{1k\Omega} + 1 \cong 50$$

$$Total\ Gain = G_1 \times G_2 \cong 5000 \qquad 4.2$$

$$dB = 20\log(Total\ Gain) \cong 74$$

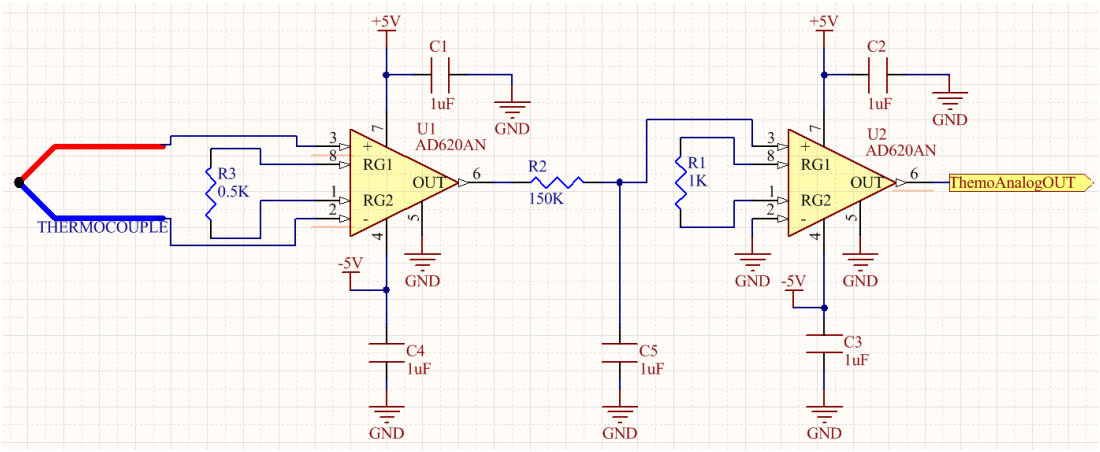

Figure 40 Thermocouple analog readout circuit

C1, C2, C3, C4 bypass capacitors are used to filter out the unwanted noisy AC signal and provide a pure DC signal for the supply inputs. Respiration frequency of adults at rest is approximately 0.3 Hz, therefore low pass filter with a 1.06Hz cut-off frequency is used to eliminate 50Hz mains noise. According to R2 and C5, cut-off frequency (f_c) is calculated in Equation 4.3.

$$f_c = \frac{1}{2\pi RC} \cong 1.06Hz \qquad 4.3$$

The effect of the low pass filter on the first stage amplification output of the thermocouple is shown in Figure 41.

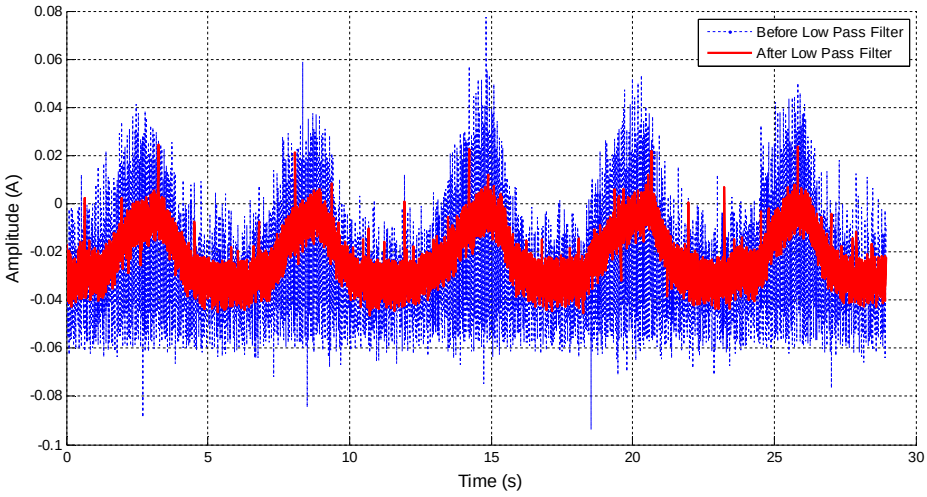

Figure 41 Effect of the low pass filter on the first stage amplification output of the thermocouple readout circuit

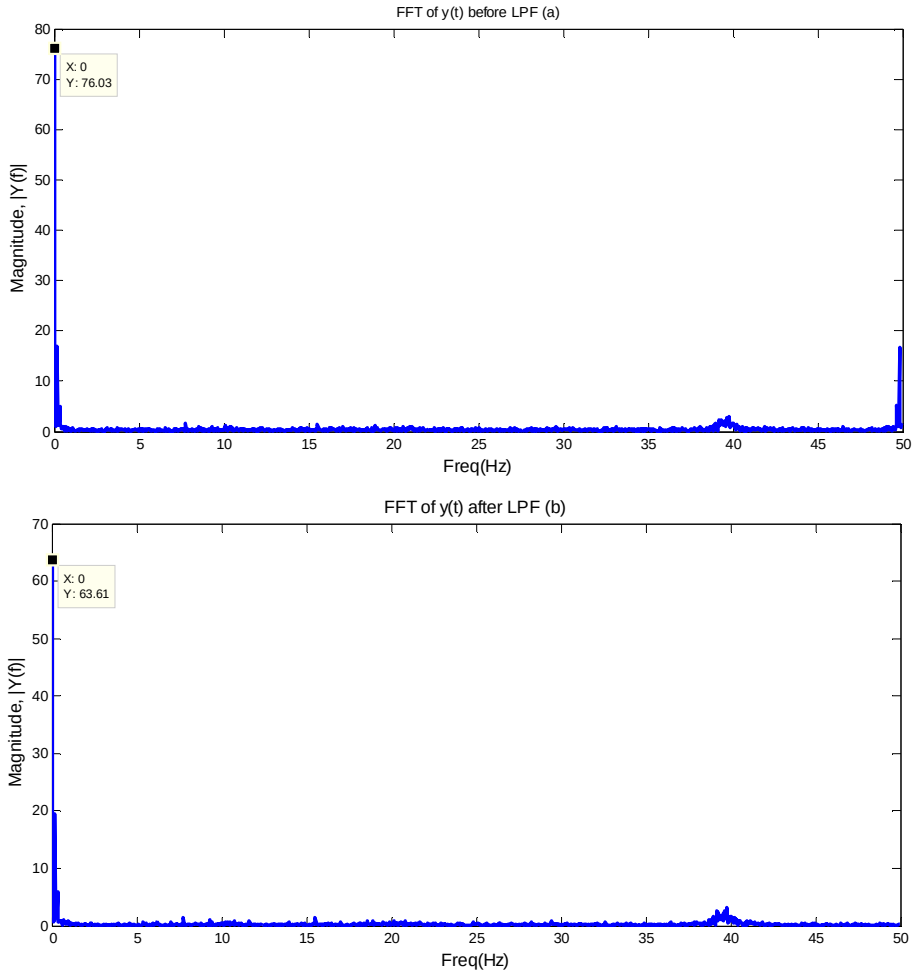

Figure 42 FFT of the respiration signal before LPF (a) and after LPF (b)

Thermocouple output after the second stage amplification is shown in Figure 43.

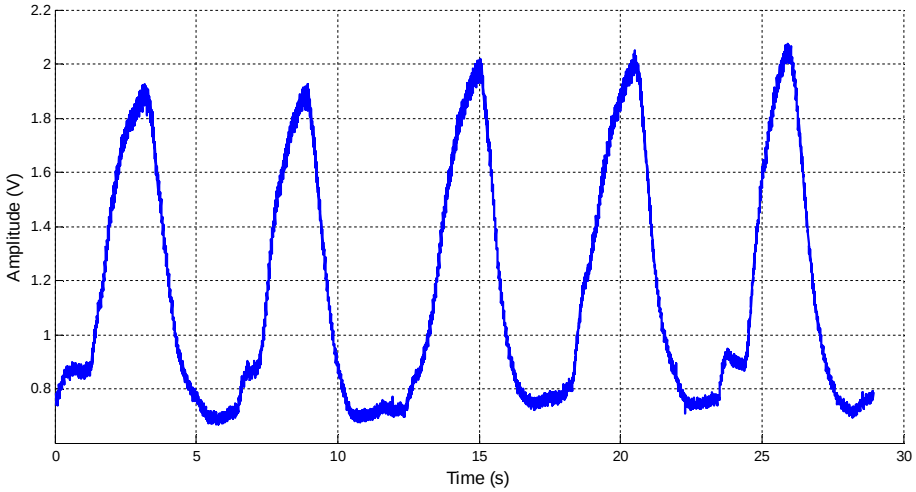

Figure 43 Thermocouple readout circuit analog output

4.3.2 Pulse Oximeter Readout Circuit Tests

PPG signal occurs at the output of the photo diode has low amplitude, noise and DC component. Therefore, it should be filtered and amplified. Passive high pass filter with ~0.6Hz cut-off frequency is used to block the DC component and low pass filter with ~3.2Hz cut-off frequency is used to eliminate high frequency noise. In the first stage of the amplification, the output of the LPF is amplified ~150 times with an operational amplifier (LM358) and also filtered by means of the op amp based active low pass filter with ~3.2Hz cut-off frequency. Filtering and the first stage amplification circuit of the pulse oximeter readout design is shown in Figure 44. Measured PPG signal after high pass filter (on TP3) and after low pass filter (on TP4) of the pulse oximeter readout circuit is shown in Figure 45.

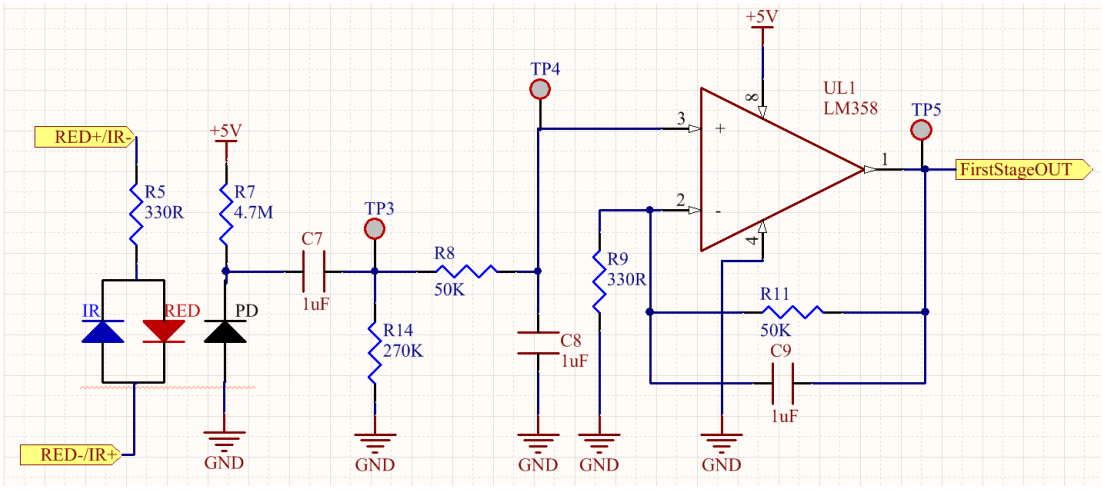

Figure 44 Filtering and first stage amplification circuit of the pulse oximeter readout design

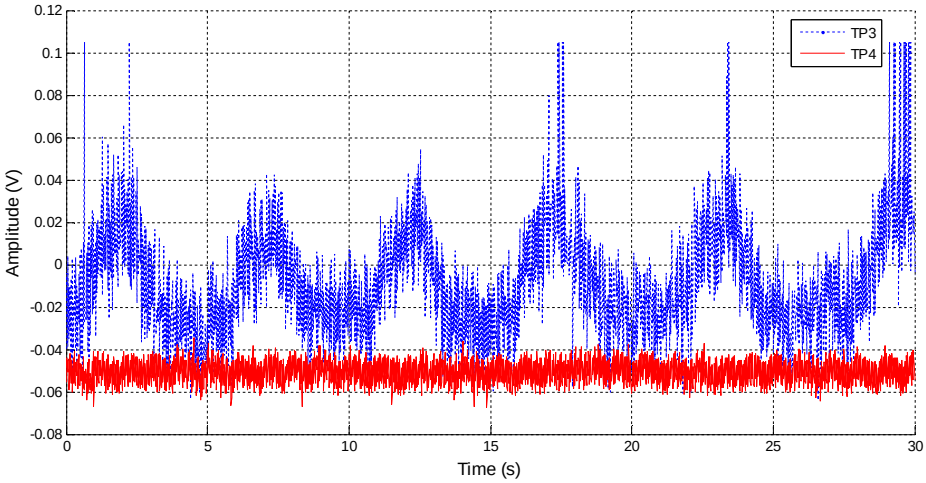

Figure 45 Measurement from TP3 (after high pass filter) and TP4 (after low pass filter) of the pulse oximeter readout circuit

Frequency domain examination of the signals on TP3 and TP4 shows that, high frequency component is removed by applying low pass filter. FFT of the PPG signal obtained from TP3 and TP4 is shown in Figure 46.

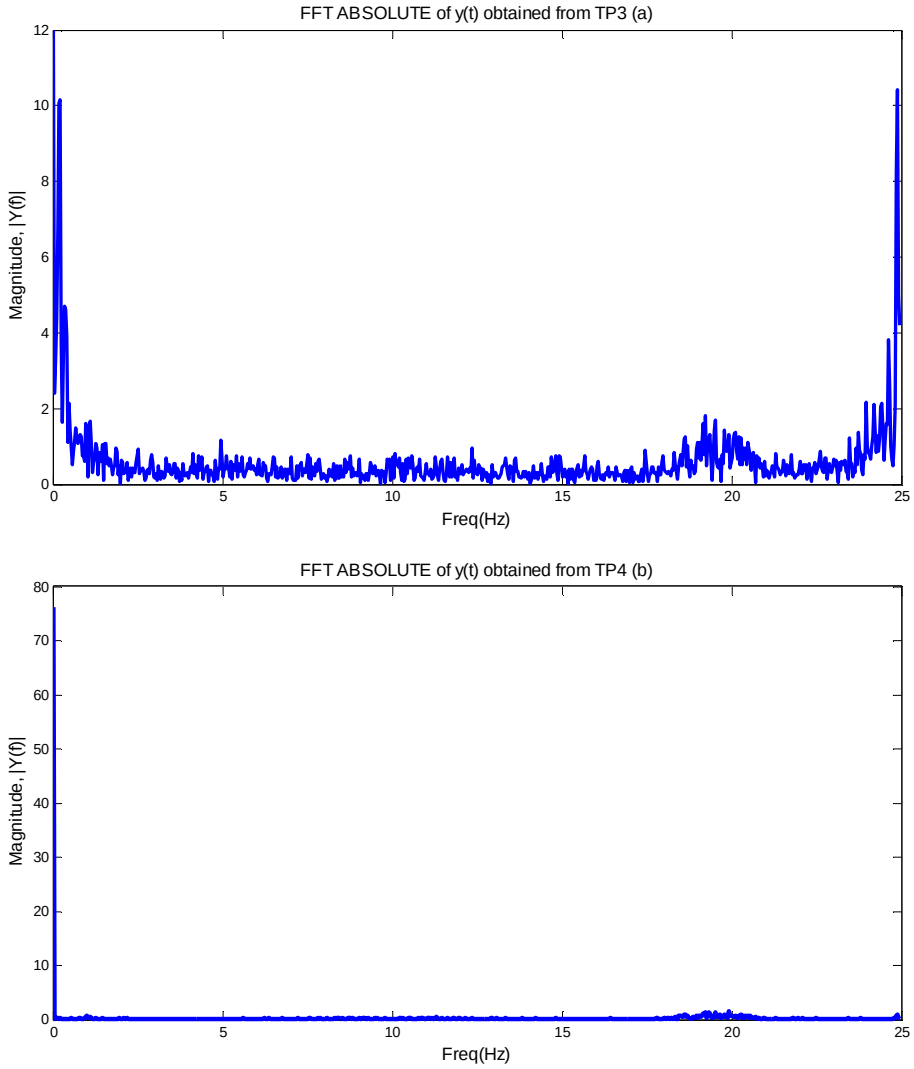

Figure 46 FFT of the PPG signal obtained from TP3 (a) and TP4 (b)

Before second stage amplification HPF with ~0.6Hz cut-off frequency is used to eliminate DC component in case of saturation problem of the op-amp and to block the respiration frequency effect on the PPG signal. Feedback capacitor on the first stage is used to create active LPF with ~3.2Hz cut-off frequency to eliminate high frequency noise, minimize peak gain, improve stability and limit bandwidth.

Output of the first stage amplification and the final output of the PPG signal are shown in Figure 47. Two stage amplification helps to obtain sharper peaks by using active low pass filter.

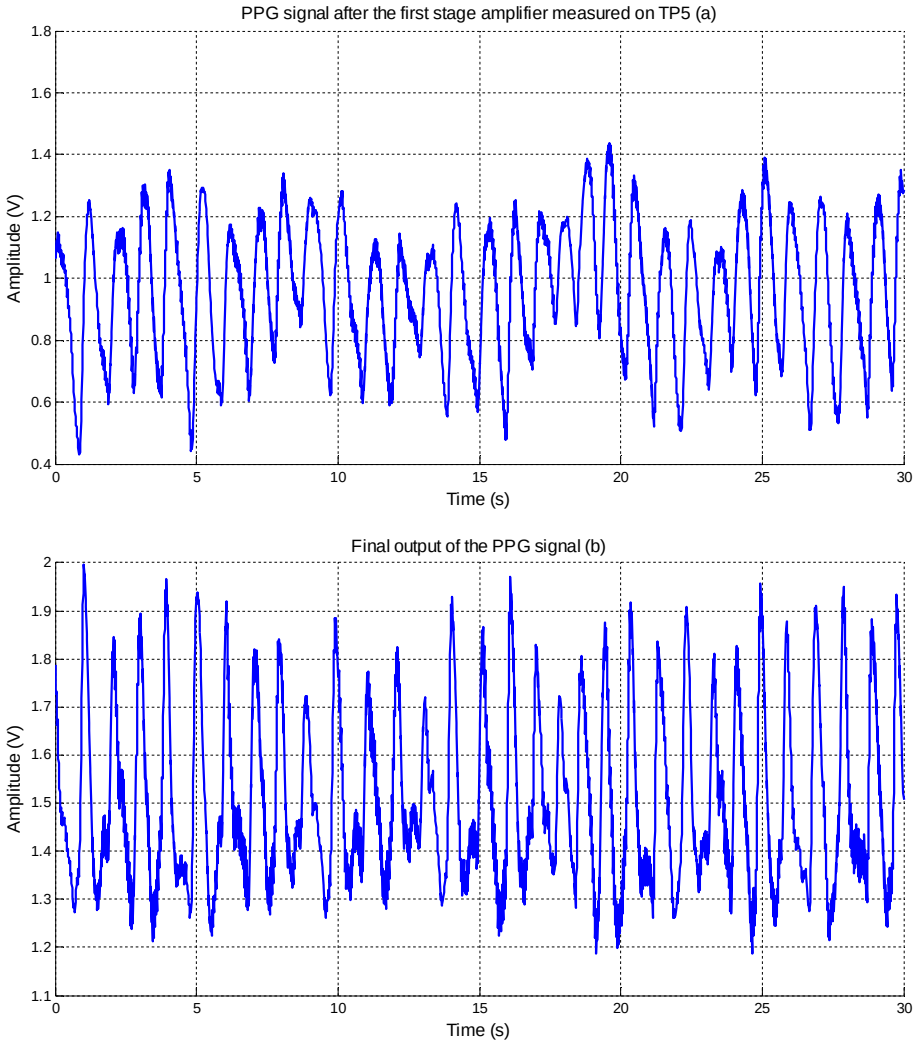

Figure 47 PPG signal after the first stage amplifier measured on TP5 (a), final output of the PPG signal (b)

Entire pulse oximeter readout circuit is shown in Figure 48.

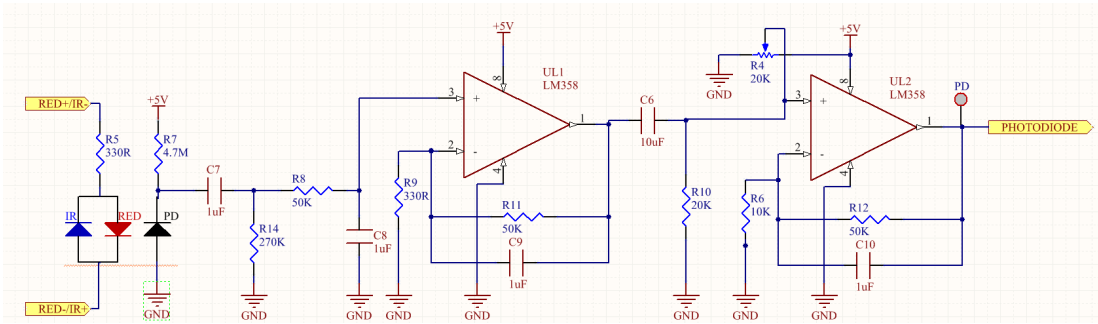

Figure 48 Pulse oximeter readout circuit

4.3.3 Magnitude Response and CMRR Measurement

The differential mode gain with respect to frequency of the thermocouple analog readout circuit is given in Figure 49.

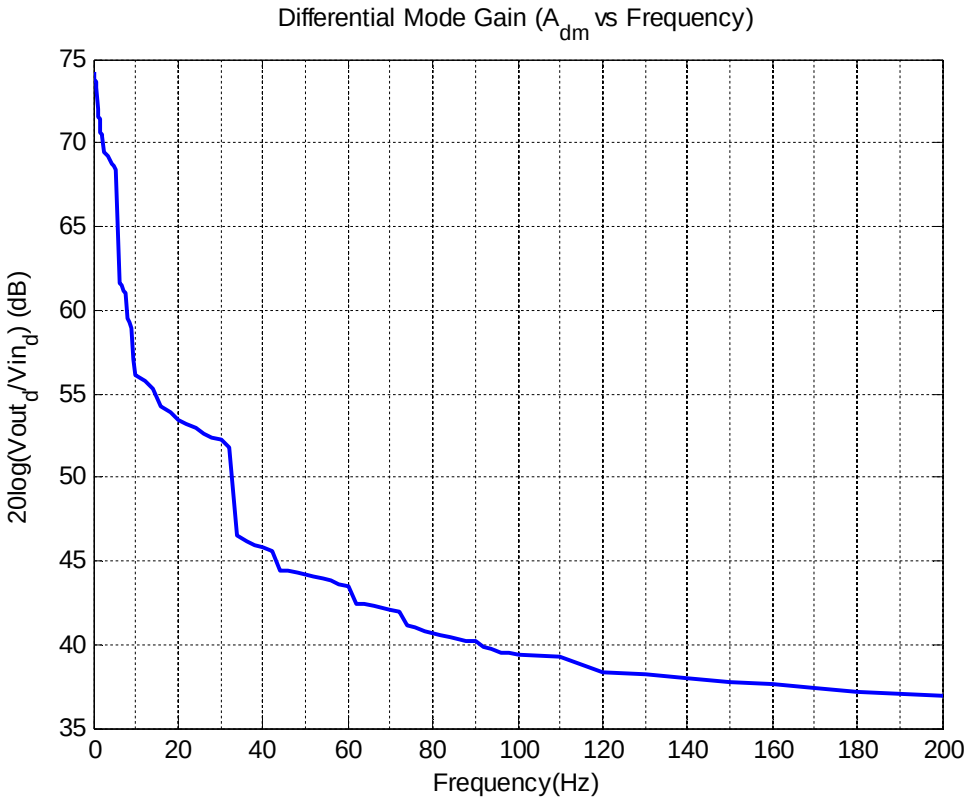

Figure 49 Magnitude response of the thermocouple analog readout circuit

It is seen from Figure 49 that the thermocouple analog readout circuit has a nonlinear differential gain for the measured frequency range. It has maximum gain between 1 and 5 Hz and the gain reduces with the increased frequency. The CMRR of the thermocouple readout circuit with respect to frequency is presented in Figure 50.

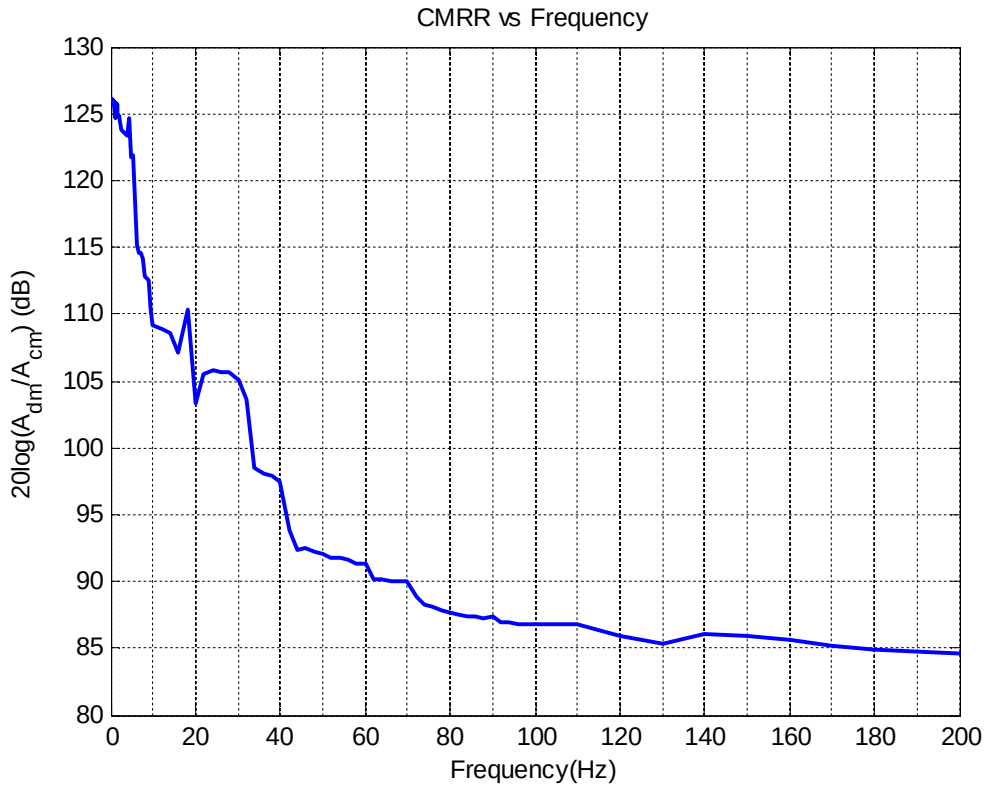

Figure 50 Common Mode Rejection Ratio (CMRR) of the thermocouple readout circuit

Measured CMRR value of the thermocouple readout circuit is approximately 92dB at 50Hz mains frequency. This value is low but it does not affect the sleep apnea detection system. Because the system is powered by the battery, therefore there is not any conduction to mains. In addition, the main frequency component of the respiration signal in adults is in the order of 0.3Hz and measured CMRR value is between 110 and 126dB in 0 to 5Hz range.

CHAPTER 5

RESULTS OF EXPERIMENTAL MEASUREMENT OF HEALTY HUMAN SUBJECTS

5.1 Introduction

In this chapter, calibration of pulse oximeter, the description of test database which consisted of healthy volunteers and the accuracy of apnea detection, heart rate and SpO_2 calculation are provided.

5.2 Calibration of the Pulse Oximeter

As stated in previous chapters, there is a need for calibration of pulse oximeter by obtaining data from healthy human volunteers. Data gathering from the volunteers is started after the approval of Applied Ethics Research Center of METU. The approval form may be found in APPENDIX C.

According to the Beer-Lambert law, R values are calculated by utilizing AC-DC values of both infrared and red lights by considering only absorbed and transmitted light. But in fact, there are also reflected and scattered light while red and infrared light transmitting through the finger to the photo diode. Therefore, most of commercial pulse oximeters are self-calibrated. In this study, a standard pulse oximeter device (MD300C12) is used to make in vitro calibration and determine coefficients a and b based on Equation 5.1. Corresponding R values to the observed standard device SpO_2 values are collected from different samples, the coefficients are determined by performing simple linear regression model using the least squares method with the following formula [57].

$$a = \frac{\sum_{i=1}^{n} S_i \sum_{i=1}^{n} R_i^2 - \sum_{i=1}^{n} R_i \sum_{i=1}^{n} R_i S_i}{n\sum_{i=1}^{n} R_i^2 - \left(\sum_{i=1}^{n} R_i\right)^2} \quad b = \frac{n\sum_{i=1}^{n} R_i S_i - \sum_{i=1}^{n} R_i \sum_{i=1}^{n} S_i}{n\sum_{i=1}^{n} R_i^2 - \left(\sum_{i=1}^{n} R_i\right)^2} \qquad 5.1$$

Where S_i is the SpO_2 value observed from the standard device, R_i is the calculated red to infrared absorption ratio, and n states the number of calibration measurements. According to the Equation 2.17 correlation between R and SpO_2 can be stated with the following linear formula:

$$SpO_2 = 99.4764 - 2.4366 \times R \qquad 5.2$$

5.3 Description of the Test Database

Test measurements are recorded from 5 people who have not got any known health disorders. Information about the subjects is given in Table 4.

Table 4 Age and gender distribution of the test records

Test Records	Age	Gender
Subject-1	27	F
Subject-2	30	M
Subject-3	37	F
Subject-4	38	M
Subject-5	29	M

While recording the data, it is requested from the subjects to place the thermocouple to their nose and the pulse oximeter to their finger and continue to breathe in a comfortable position. Experimental measurement setup of a subject is shown in Figure 51. Position of the thermocouple probe in the nostrils, placement of the pulse

oximeter probe to the finger, the sleep apnea detection kit and an android device is also shown in Figure 51.

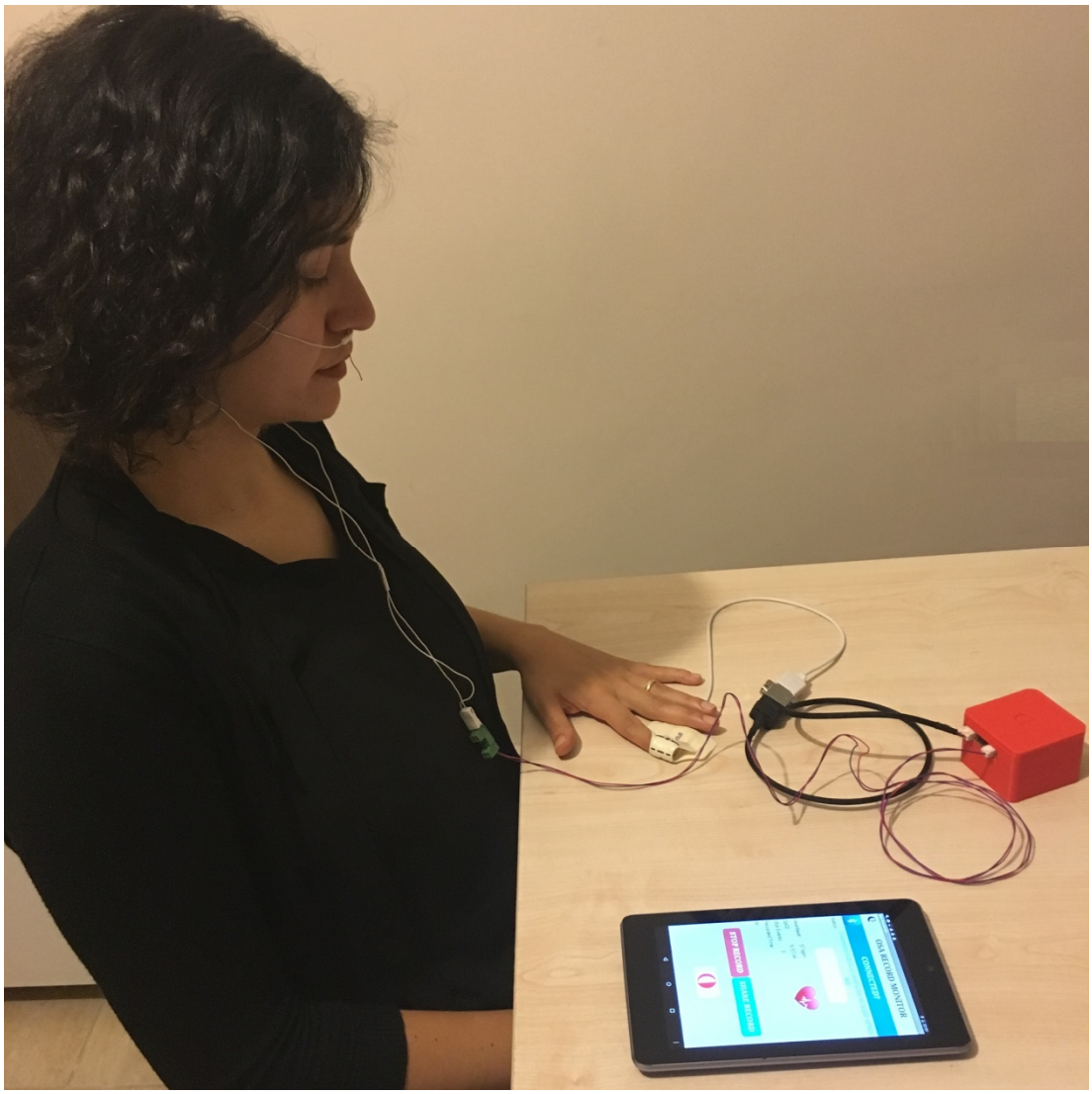

Figure 51 Experimental measurement setup of a subject

During measurements, subjects are requested to hold their breath more than 10 seconds and continue to breathe normally. Annotations of the test scenario are shown in Table 5. According to the test scenario, there are apnea simulations which imply the respiration cessation parts longer than 10 seconds are shown between 1.50-2.05, 3.00-3.12 and 3.50-4.10 minutes. In order to test the sleep apnea detection algorithm

accuracy, it is requested from the subjects to hold their breath approximately 5 seconds. These 5 seconds cessation parts occur between 4.30-4.35 and 4.45-4.50 minutes. These cessations parts are annotated just a holding breath not an apnea simulation.

Table 5 Annotations of the test scenario

Test Time	**Annotations**
0-40 sec	Normal respiration
40. sec	Calibration starts for thermocouple data
40-60 sec	Calibration duration with normal respiration
60. sec	Calibration ends
1.0 - 1.50 min	Continue normal respiration
1.50 - 2.05 min	Holding breath (apnea simulation)
2.05 - 3.00 min	Continue normal respiration
3.00 – 3.12 min	Holding breath (apnea simulation)
3.12 – 3.50 min	Continue normal respiration
3.50 – 4.10 min	Holding breath (apnea simulation)
4.10 – 4.30 min	Continue normal respiration
4.30 – 4.35 min	Holding breath
4.35 – 4.45 min	Continue normal respiration
4.45 – 4.50 min	Holding breath
4.50 – 5.00 min	Continue normal respiration

In Figure 52, thermocouple readout recording of Subject-2 is shown. It is seen that three apnea simulation parts are detected according to the calculated threshold crossing points. Approximately 5 seconds cessation parts are also observed in the figure.

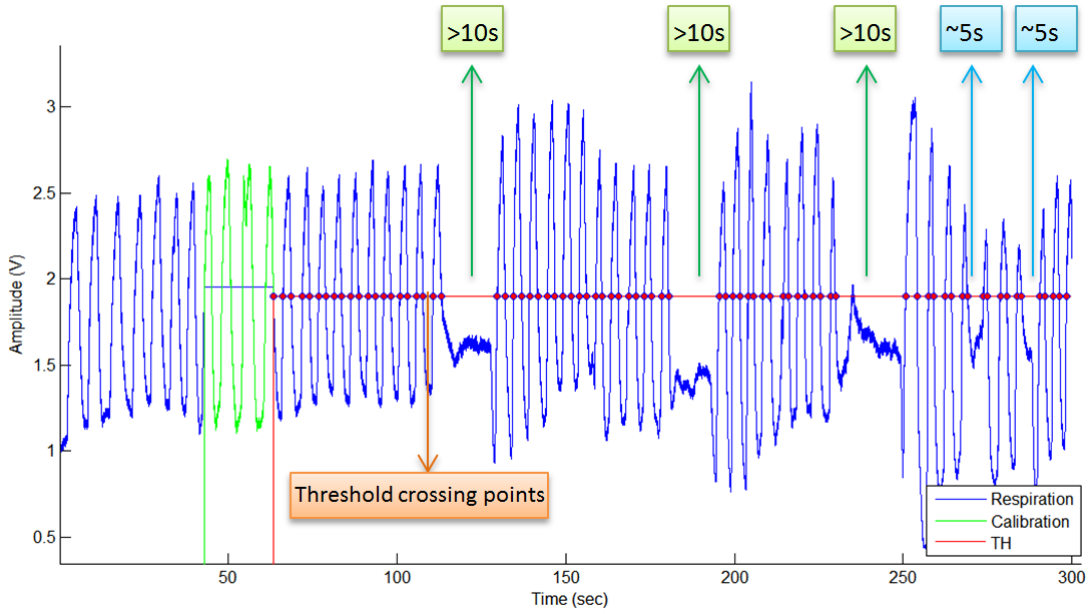

Figure 52 Thermocouple readout recording of Subject-2, blue is thermocouple data, green is thermocouple data during calibration and red one is the threshold value calculated from the calibration signal

Photodiode output obtained from ADC data of the infrared and red signal and the calculated peak signal of the infrared signal is shown in Figure 53.

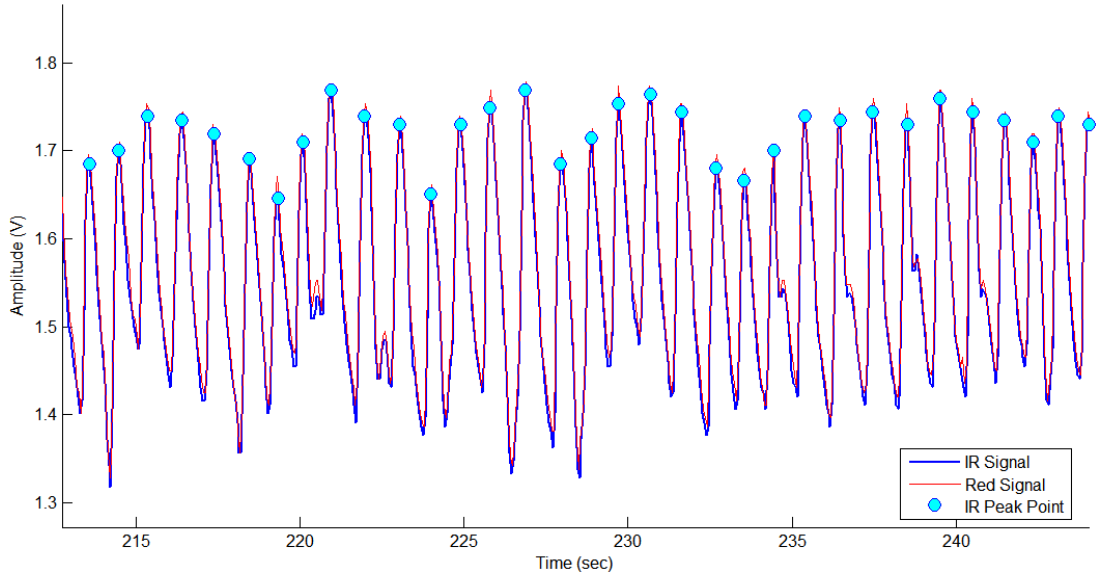

Figure 53 Red and infrared signal obtained from ADC output of the photodiode

5.4 Accuracy of the System

According to the test measurements that comprises of 5 volunteer, respiratory and pulse oximeter data is acquired by means of ARM processor through the designed analog circuit and is recorded in the mobile device by connecting ARM processor and mobile device via Bluetooth. During recording of the measurements, sleep apnea, heart rate and SpO_2 are determined simultaneously. According to the annotations of the test scenario, ground truth analysis is implemented to examine accuracy. For ground truth analysis initial supervised classification is applied and this classification results are considered. If the annotation of the test scenario shown in Table 5 is considered, apnea number should be 3 after the test of each subject. In addition, approximately 5 second cessation parts of the test records should not be labelled as apnea. The sensitivity (also called the true positive rate) and specificity (also called the true negative rate) of the system is determined according to the correct classification or correct rejection of apnea parts in the test records. Regarding to the supervised classification of each test records, number of true positives (TP) is 3, number of false positives (FP) is 0, number of true negatives (TN) is 2 and number of false negatives (FN) is 0.

$$Sensitivity = \frac{TP}{TP + FN}$$
$$Specificity = \frac{TN}{TN + FP} \qquad 5.3$$

According to Equation 5.3, the system's sleep apnea detection sensitivity and specificity value is calculated as 100%. The reason why the value of sensitivity and specificity is so high is the test scenario. Because the test scenario contains 5 minutes of data of 5 subjects which is obtained in a controlled environment. This value may reduce if the test duration is extended and the number of subjects is increased. Also, if the test data is collected not only from normal people but also from people with suspected sleep apnea, the value may also decrease.

As it is stated in 3.7, heart rate calculation is applied according to the peak detection algorithm and by using threshold crossing algorithm sleep apnea is detected. In the test records, there are a few false positive values for heart rate and threshold crossing point calculation and this affects the accuracy. Accuracy is calculated according to the Equation 5.4.

$$Accuracy = \frac{TP + TN}{TP + FP + FN + TN} \qquad 5.4$$

Accuracy of measurements by using the selected peak detection and threshold crossing algorithms is given in Table 6.

Table 6 Accuracy of the experimental result

	Subject-1	**Subject-2**	**Subject-3**	**Subject-4**	**Subject-5**
Number of Apnea>10 sec	100%	100%	100%	100%	100%
Heart Rate	99.75%	100%	100%	96.62 %	98.9%
Threshold Crossing Point	97.1%	99%	95.8%	100%	96.7%

Accuracy of SpO_2 calculation of the system is compared with the measurements of the standard device and shown in Table 7. During the comparison, R value of the designed system is observed simultaneously with the measured SpO_2 value of the standard device.

Table 7 Accuracy of the SpO_2 calculation

Record Name	**R**	**Standard Device**	**SpO_2=99.4764 – 2.4366*R**
Subject-1	1	98 %	97.03 %
Subject-2	1,038	98 %	96.94 %
Subject-3	0.975	98 %	97.1 %
Subject-4	0.99	99 %	99.24 %
Subject-5	0.996	98 %	99.23 %

CHAPTER 6

CONCLUSION

In this chapter, the thesis study is summarized together with all the features, necessity of the work and the experimental results. The issues which may be developed by future studies are mentioned.

6.1 General Observations and Discussions

Sleep apnea is a common sleep disorder which can be observed in both children and adults. During sleep apnea, breathing stops. If this takes quite long, it can be fatal. Besides, sleep deprivation due to several pauses through the night causes many daytime symptoms to the patients such as headache, high blood pressure, depression, carelessness, and fatigue. Despite several treatment options, there is only one gold standard for the detection of sleep apnea, which is PSG. But taking a PSG exam is considered to be difficult, expensive and time consuming.

The motivation of this study is to design a portable, low cost and user friendly device to detect sleep apnea which offers the possibility of sleep testing in one's own bed where he/she is most comfortable. Thus, by eliminating the necessity to stay overnight in sleep laboratory rooms, this device remedies one of the most disturbing sides of the standard PSG exams.

The device is designed for preclinical applications such as home sleep testing. By this way, there is not any need to wait for sleep laboratory rooms for sleep testing and screening for sleep apnea syndrome can be detected.

As it is stated in CHAPTER 1, sleep apnea has three types as obstructive, central and mixed. Obstructive sleep apnea occurs when there is partial or complete collapse of the upper air path by the soft tissue in the rear of the throat. If the respiratory muscles could not receive the appropriate neural control signal, central sleep apnea occurs. During the central sleep apnea, chest and brain effort is not observed in contrast to obstructive sleep apnea. In order to classify sleep apnea types, chest or brain effort should be considered by using sensors for abdominal, chest or brain signals. In this system temperature sensor is used for nasal airflow and pulse oximeter sensor is used for blood oxygen saturation measurements. Therefore, classification of the sleep apnea types is not applicable for this system. Only sleep apnea which is defined as the cessation of breath at least 10 seconds during the sleep is detected with the proposed system.

The system uses an Android device for monitoring the required information and has a wireless data sharing and recording options which make the system lightweight and easy to use. In addition, the system is able to share the necessary information with patients and doctors for the duration of the whole sleep cycle.

With a total cost of 35$, the designed sleep apnea detection device is also cost effective when compared to PSG exam. It is estimated that this cost can be reduced to 10-15$ by mass production.

The system detects apneic attack by analysing the respiratory signals obtained from oronasal thermocouple which senses the airflow according to the temperature variations. Considering the difference of body temperature, respiratory effort, and position of the sensor, auto calibration is made possible for each patient. According to the calculated threshold value, threshold detection algorithm is applied and sleep apnea is detected.

Pulse oximeter is used as an alternative sensor to calculate SpO_2 and heart rate. If the thermocouple sensor drops or it is not placed properly to the nose, the specialists may examine the SpO_2 and heart rate records to comprehend the apneic attacks. Using peak detection algorithm based on photodiode output of infrared LED, SpO_2 and heart rate are calculated.

In order to test the performance of the system on humans, a test database is formed with the approval of the Applied Ethics Research Committee of METU. Calibration of pulse oximeter is applied by collecting data from 10 people by utilizing a standard oximeter and the designed device. Simple linear regression model is performed to obtain a linear relation between R and SpO_2. According to the calculated linear equation, SpO_2 and heart rate are calculated and compared with the standard device. The results show that SpO_2 and heart rate calculations are approximately 99% accurate.

Test database is also used for performance assessment of apnea detection. The accuracy of the results is examined by the method of ground truth analysis. Consistent with the results, sleep apnea with a longer duration of 10 seconds is detected with 100% accuracy and the threshold crossing point is calculated with about 98% accuracy. The system also has the ability to ring the alarm of the Android device if the apnea takes longer than 30 seconds in order to avoid fatal risks.

Accuracy of the experimental results shows the performance of the system according to the determined test scenario on limited number of subjects. There are several studies by using portable home sleep testing devices. Every device uses different sensors as the indicator signal like EEG, nasal pressure, microphone, pulse oximeter. While the accuracy of the system is specified, no comparison is made between the other portable sleep apnea devices and the designed sleep apnea kit.

6.2 Future Work

The thesis can be further developed by additional studies on the following issues:

- The designed apnea detection and SpO_2 or heart rate calculation algorithms are applicable for time domain features. Frequency domain signal frequency algorithms may be implemented and digital filtering techniques can be used to improve the performance of the system by considering the processor capabilities.

- The printed circuit board is produced as two-layer PCB on LPKF rapid PCB prototyping machine, component placement and soldering are performed by hand. An enhanced performance may be achieved by manufacturing PCB as four-layer, applying conformal coating and using pic and place machines for component placement. Dimension of the circuit may be reduced substantially by using small package SMT components.

- Finally, using additional sensors, detection of other breathing abnormalities other than sleep apnea; such as hypopnea, Cheyne-Strokes breathing, hypoventilation, etc. may be accomplished.

6.3 Publications during MSc. Study

D. Demirkol Çakmak, B. M. Eyüboğlu, "Portable Obstructive Sleep Apnea Detection and Monitoring", in XIV Smart Biomedical and Physiological Sensor Technology, Proc. Of SPIE Vol. 10216, 1021606.

REFERENCES

[1] J.H. Peter, T. Podzus, P.V. Wichert, Sleep related disorders and internal diseases, New York: Springer, 1987, pp. 101-107.

[2] P. Lavie, P. Herer, R. Peled, I.Berger, N. Yoffe, J. Zomer, A.E. Rubin, "Mortality in sleep apnea patients: a multivariate analysis of risk factors," *Sleep,* vol. 18, no. 3, pp. 149-157, 1995.

[3] J. Tu, K. Inthavong, G. Ahmadi, Computational fluid and particle dynamics in the human respiratory system, Spiringer, pp. 19-44.

[4] OpenClipart-Vectors images/ 27444, "Pixabay," [Online]. Available: https://pixabay.com/en/anatomy-lungs-breathing-human-145696/. [Accessed 09 April 2018].

[5] Clker-Free-Vector-Images / 29607, "Pixabay," [Online]. Available: https://pixabay.com/en/health-labelled-science-organic-41510/. [Accessed 09 04 2018].

[6] J. Webster, Design of pulse oximeters, Bristol: IOP Publishing, 1997.

[7] A.C. Guyton, J.E. Hall, Textbook of medical physiology, Philadelphia: Elsevier Saunders, 2006.

[8] [Online]. Available: https://sleepapnea.org/learn/sleep-apnea/. [Accessed 24 February 2017].

[9] T. Young, P.E. Peppard, D.J. Gottlieb, "Epidemiology of obstructive sleep apnea, a population health perspective," *American Journal of Respiratory and Critical Care Medicine,* vol. 165, 2002.

[10] J.G. Park, K. Ramar, E.J. Olson, "Updates on definition, consequences and management of obstructive sleep apnea," *Mayo Clinic Proceedings,* vol. 86, no. 6, pp. 549-555, 2001.

[11] D. Priyalakshmi, "Association between periodontitis and obstructive sleep apnea," *Research in Humanities and Social Science,* vol. 2, no. 11, pp. 37-45, 2014.

[12] "Diseases and Conditions - Sleep Apnea," [Online]. Available:

https://www.mayoclinic.org/diseases-conditions/sleep-apnea/basics/definition/con-20020286. [Accessed 1 December 2017].

[13] K. Becker, J.M. Wallace, “Central sleep apnea: follow-up,” Medscape. [Online]. [Accessed 1 December 2017].

[14] R. Wilkin, Clinical assessment in respiratory care, st Louis: MO: Mosby, 1985, pp. 268-272.

[15] R. Martin, Cardiorespiratory disorders during sleep, Mount Kisco: NY: Futura, 1990, pp. 123-169.

[16] J. Jin, E. Sanchez-Sinencio, “A home sleep apnea screaning device with time domain signal processing and autonomous scoring capability,” vol. 9, no. 1, 2014.

[17] N. Punjabi, “The epidemiology of adult obstructive sleep apnea,” vol. 5, 2008.

[18] T.Young, L. Evans, L. Finn, M.Palta, “Estimation of the clinically diagnosed proportion of sleep apnea syndrome in middle-aged men and women,” *Sleep*, vol. 20, no. 9, pp. 705-6, 1997.

[19] L.J. Findley, J.W. Weiss, E.R. Jabour, “Drivers with untreated sleep apnea a cause of death and serious injury,” vol. 7, 1991.

[20] H.K. Yaggi, J. Concato, W.N. Kernan, J.H. Lichman, L.M. Brass, V. Mohsenin, “Obstructive sleep apnea as a risk factor for stroke and death,” vol. 353, 2005.

[21] C. Sunitha, S. Aravindkumar, “Obstructive sleep apnea: clinical and diagnostic features,” vol. 20, 2009.

[22] N. Oliver, F. Flores-Mangas, “HealthGear: automatic sleep apnea detection and monitoring with mobile phone,” *Journal of Communications,* vol. 2, no. 2, 2007.

[23] A. Garde, P. Dehkordi, D. Wensley, J.M. Ansermino, G.A Dumont, “Pulse oximetry recorded from the phone oximeter for detection of obstructive sleep apnea events with and without oxygen desaturation in children,” 2015.

[24] D.Falie, M. Ichim, “Sleep monitoring and sleep apnea event detection using 3D camera,” in *International Conference on Communications (COMM)*, 2010.

[25] C.Wang, A. Ahmed, A. Hunter, “Vision analysis in detecting abnormal

breathing activity in application to diagnosis of obstructive sleep apnea," in *EMBS*, New York, USA, 2006.

[26] G. Sannino, I. De Falco, D. De Pietro, "Detecting obstructive sleep apnea events in a real-time mobile monitoring system through automatically extracted sets of rules," in *IEEE HEALTHCOM*, 2013.

[27] G. Surrel, S. Murali, "Low power wearable system for real time screening of obstructive sleep apnea," *IEEE Computer Society Annual Symposium on VLSI*, vol. 2, no. 16, 2016.

[28] T. Penzel, J. McNames, A. Murray, P. Chazal, G. Moody, and B. Raymond, "Systematic comparison of different algorithms for apnoea detection based on electrocardiogram recordings," *Medical & Biological Engineering & Computing Journal*, vol. 40, no. 4, pp. 402-407, 2002.

[29] M. Mendez, D. Ruini, O. Villantieri, M. Matteucci, T. Penzel, and A. Bianchi, "Detection of sleep apnea from surface ECG based on features extracted by an autoregressive model," in *Engineering in Medicine and Biology Society (EMBS)*, 2007.

[30] R. Brugarolas, J.M. Valero-Sarmiento, A. Brna, "Wearable SpO2 and sleep posture monitoring system for obstructive sleep apnea patients," 2015.

[31] S. Algassim, M. Ganesh, S. Khoja, M. Zaidi, F. Aloul, A. Sagahyroon, "Sleep apnea monitoring using mobile phones".

[32] A. Mudvari, T. Ning, "Respiration estimation and apnea detection using fuzzy logic," in *Engineering in Medicine and Biology Society (EMBC)*, 2017.

[33] K. Nepal, E. Biegeleisen, T. Ning, "Apnea detection and respiration rate estimation through parametric modelling," 2002.

[34] Y.Zhao, H. Zhang, W. Liu, S. Ding, "A snoring detector for OSAHS based on patient's individual personality," in *Awereness Science and Technology (iCAST)*, 2011.

[35] A. Yadollahi, Z. Mousaavi, "Acoustic obstructive sleep apnea detection," in *IEEE Engineering in Medicine and Biology Society (EMBS)*, Minnesota, 2009.

[36] O. Sechang, K. Hyeokjun, and V. Vijay, "Ubiquitous health monitoring system for diagnosis of sleep apnea with Zigbee network and wireless LAN,"

Nanotechnology in engineering and medicine, vol. 2, no. 2, 2011.

[37] R.B. Berry, R. Budhiraja, D.J. Gottlieb, D. Gozal, C. Iber, V.K. Kapur, C.L. Marcus, R. Mehra, S. Parthasarathy, S.F. Quan, S. Redline, K.P. Strohl, S.L. Ward Davidson, M.M. Tangredi, "Rules for scoring respiratory events in sleep: update of the 2007 AASM manual for the scoring of sleep and associated events. Deliberations of the sleep apnea definitions task force of the American Academy of Sleep Medicine," *Journal of Clinical Sleep Medicine (JCSM),* vol. 15, no. 8, pp. 597-619, 2012.

[38] Y. Pole, "Evolution of the pulse oximeter," *International Congress Series,* vol. 1242, pp. 137-144, 2002.

[39] G.M. Azmal, A. AI-Jumaily, M. AI-Jaafreh, "Continuous measurement of oxygen saturation level using photoplethysmograph signal," 2006.

[40] W.G. Zijlstra, A. Buursma, H.E. Falke, J.F. Catsburg, "Spectrophotometry of hemoglobin: absorption spectra of rat oxyhemoglobin, deoxyhemoglobin, carboxyhemoglobin, and methemoglobin," *Comparative Biochemistry and Physiology Part B: Comparative Biochemistry,* vol. 107, pp. 161-166, 1994.

[41] M. Nitzan, A. Babchenko, B. Khanokh, "Measurement of oxygen saturation in venous blood by dynamic near infrared spectroscopy," vol. 2, 2000.

[42] S.J. Barker, K.K. Tremper, "Pulse oximetry," vol. 70, 1989.

[43] J.P. de Kock, L. Tarassenko, "Pulse oximetry: theoretical and experimental models," *Medical and Biological Engineering and Computing,* vol. 31, no. 3, pp. 291-300, 1993.

[44] S. Reddy, "Thermocouple working principle," 25 December 2015. [Online]. Available: http://instrumentationtools.com/thermocouple-working-principle/. [Accessed 21 February 2017].

[45] A.W Van Herwaarden, P.M. Sarro, "Thermal sensors based on the Seebeck effect," vol. 10, 1986.

[46] R. Swanson, "Thermocouples and thermistors," vol. 19.4, 2010.

[47] B.B. Winter, J.G. Webster, "Reduction of interference due to common mode voltage in biopotential amplifiers," vol. 30, 1983.

[48] J. M. Fiore, Operational amplifiers & linear integrated circuits: theory and application, James M. Fiore via dissidents, 2017.

[49] “IEEE 802.15 WPAN Task Group 1 (TG1),” [Online]. Available: http://www.ieee802.org/15/pub/TG1.html. [Accessed 14 January 2018].

[50] “SHHS Polysomnography Database,” [Online]. Available: https://physionet.org/pn3/shhpsgdb/. [Accessed 23 01 2018].

[51] A. Rodriguez-Molinero, L. Narvaiza, J. Ruiz, C. Galvez-Barron, “Normal respiratory rate and peripheral blood oxygen saturation in the elderly population,” vol. 61, no. 12, 2013.

[52] C. Chen, Signal processing handbook, New York: Dekker, 1988.

[53] K. Barrett, H. Brooks, S. Boitano, S. Barman, Ganong's review of medical physiology, Mc Graw Hill Medical, 2010.

[54] S.R. Dumpala, S.N. Reddy, S.K. Sarna, “An algorithm for the detection of peaks in biological signals,” *Computer Programs in Biomedicine*, vol. 14, pp. 249-256, 1982.

[55] American Heart Association, “Target heart rates,” 12 October 2016. [Online]. Available: http://www.heart.org/HEARTORG/HealthyLiving/PhysicalActivity/Target-Heart-Rates_UCM_434341_Article.jsp#.WLXSmm_yipo. [Accessed 24 February 2017].

[56] American Association of Sleep Technologists, “Out of center sleep testing (OCST),” AAST, 2012.

[57] S. Matviyenko, “Pulse oximeter standard, AN2313,” cypress Perform, 2010.

APPENDIX A

MIT APP INVENTOR BLOCKS

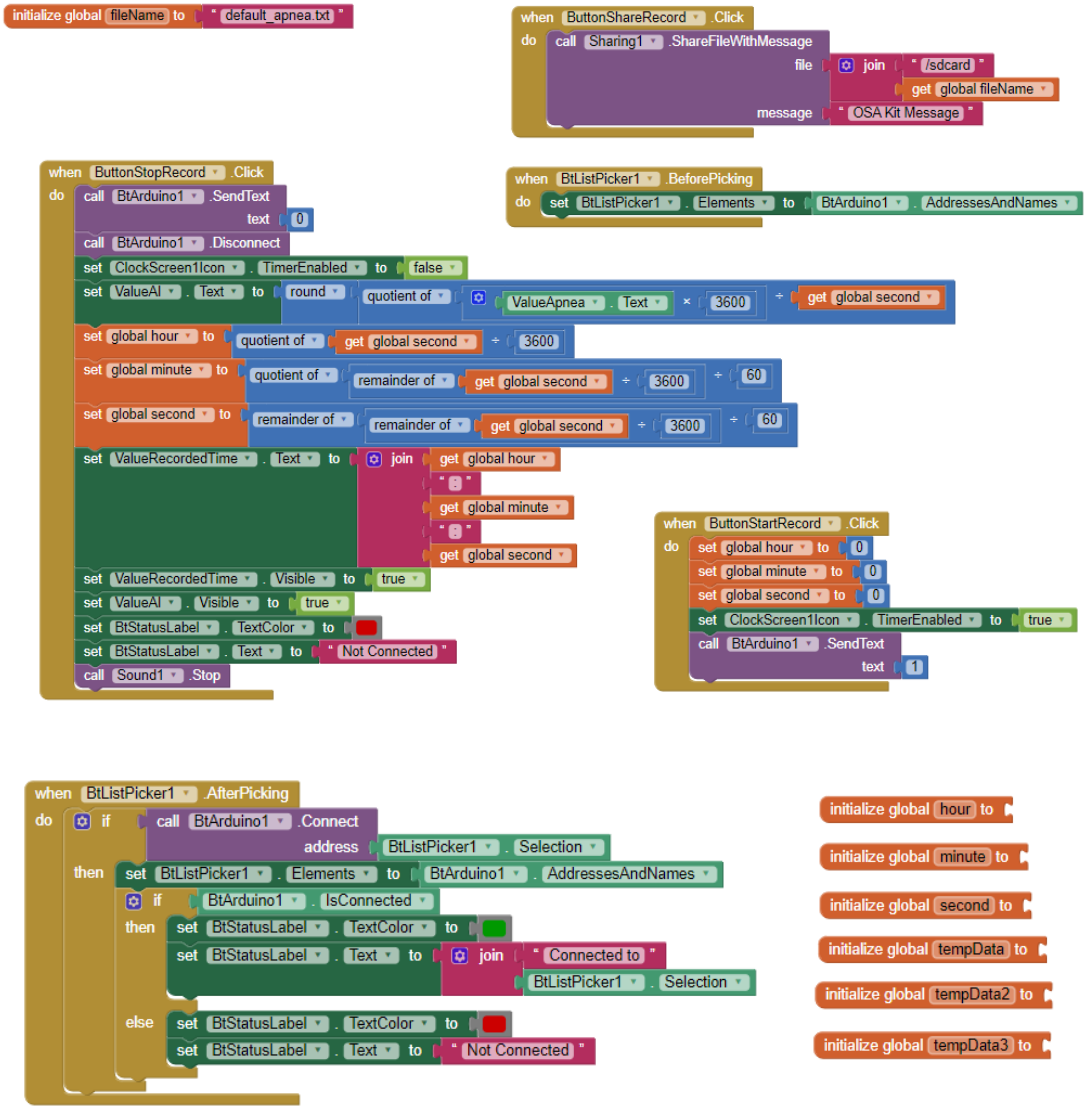

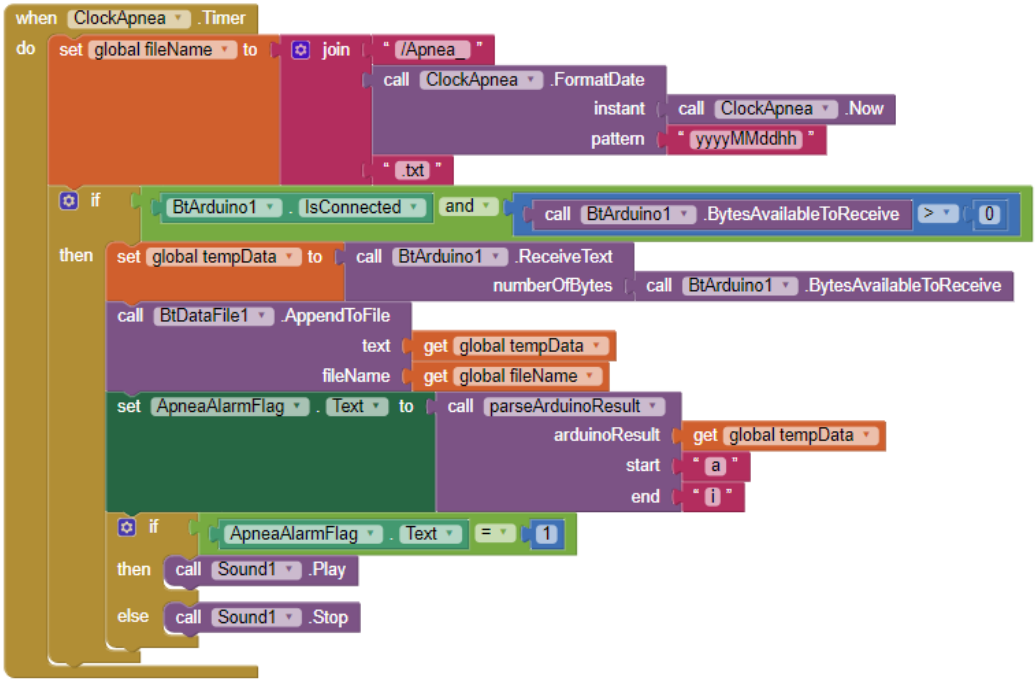
when ClockApnea .Timer
do set global fileName to join " /Apnea_ "
call ClockApnea .FormatDate
instant call ClockApnea .Now
pattern " yyyyMMddhh "
" .txt "
if BtArduino1 . IsConnected and call BtArduino1 .BytesAvailableToReceive > 0
then set global tempData to call BtArduino1 .ReceiveText
numberOfBytes call BtArduino1 .BytesAvailableToReceive
call BtDataFile1 .AppendToFile
text get global tempData
fileName get global fileName
set ApneaAlarmFlag . Text to call parseArduinoResult
arduinoResult get global tempData
start " a "
end " j "
if ApneaAlarmFlag . Text = 1
then call Sound1 .Play
else call Sound1 .Stop

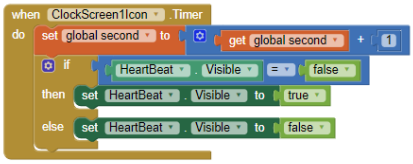
when ClockScreen1Icon .Timer
do set global second to get global second + 1
if HeartBeat . Visible = false
then set HeartBeat . Visible to true
else set HeartBeat . Visible to false

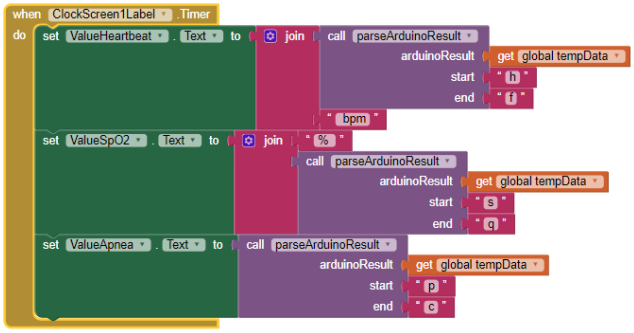
when ClockScreen1Label .Timer
do set ValueHeartbeat . Text to join call parseArduinoResult
arduinoResult get global tempData
start " h "
end " i "
" bpm "
set ValueSpO2 . Text to join " % "
call parseArduinoResult
arduinoResult get global tempData
start " s "
end " q "
set ValueApnea . Text to call parseArduinoResult
arduinoResult get global tempData
start " p "
end " c "

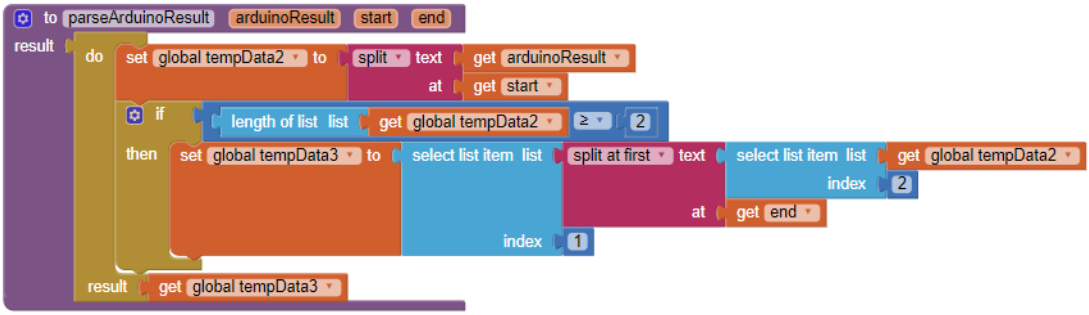
to parseArduinoResult arduinoResult start end
result
do set global tempData2 to split text get arduinoResult
at get start
if length of list list get global tempData2 ≥ 2
then set global tempData3 to select list item list split at first text select list item list get global tempData2
index 2
at get end
index 1
result get global tempData3

APPENDIX B

BILL OF MATERIALS (BOM) OF SLEEP APNEA DETECTION AND MONITORING SYSTEM

Designator	Description	Comment	Quantity	Supplier	Price ($)	Supplier Part Number
S1	Thermocouple Sensor	Salter Labs Pneumo THERM	1	tri-anim	13.5	77-5800T-0-10
S2	Pulse Oximeter Sensor	Nellcor Disposable	1	ebay	4.39	253244913549
J1_12, J2_12	ARM Processor	Arduino Pro Mini	1	direnc.net	2.9	DSTK0749
CN2	Bluetooth Module	HC-05	1	direnc.net	5.28	DSTK1507
U1, U2	Instrumentation Amplifier	AD620ANZ	2	components-shop	3.884	AD620ANZ
U3	Operational Amplifier	LM358N	1	components-shop	0.161	LM358N
I2	DC-DC Converter	LTC3525	1	components-shop	0.744	LTC3525ESC6-5#TRPBF
I1	DC-DC Converter	ICL7660SCBAZ	1	components-shop	0.292	ICL7660SCBAZ-T
CN1, CN4	Connector	Molex 2 pin header	2	digikey	0.007	0022045032-ND
CN3	Connector	Molex 4 pin header	1	digikey	0.08	S9448-ND
FT_5	Connector	5 pin header	1	digikey	0.06	8614000051LO1231-ND
R1	Resistor	2KΩ	1	digikey	1	
R2, R15	Resistor	1KΩ	2			
R3	Resistor	50KΩ	1			
R4, R8	Resistor	330Ω	2			
R5	Resistor	4.7MΩ	1			
R6	Resistor	10KΩ	1			

R7, R10, R11	Resistor	50KΩ	3			
R9	Resistor	20KΩ	1			
R12, R14, R18	Resistor	0Ω	3			
R13	Resistor	270KΩ	1			
R16	Resistor	150KΩ	1			
R17	Resistor	0.5KΩ	1			
C1, C2	Capacitor	10uF	2			
C3, C7	Capacitor	10uF	2			
C4, C5, C8, C9, C10, C11, C12, C13, C14, C15, C16, C17	Capacitor	1uF	12			
L1	Inductor	10uH	1			
TOTAL					**≈36**	

APPENDIX C

CONFIRMATION OF APPLIED ETHICS RESEARCH CENTER

UYGULAMALI ETİK ARAŞTIRMA MERKEZİ
APPLIED ETHICS RESEARCH CENTER

ORTA DOĞU TEKNİK ÜNİVERSİTESİ
MIDDLE EAST TECHNICAL UNIVERSITY

ÇUMLUPINAR BULVARI 06800
ÇANKAYA ANKARA/TURKEY
T: +90 312 210 22 91
F: +90 312 210 79 59
www.ueam.metu.edu.tr

12 EKİM 2016

Sayı: 28620816 / 389

Konu: Değerlendirme Sonucu

Gönderilen: Prof.Dr. B.Murat EYÜBOĞLU
Elektrik- Elektronik Mühendisliği

Gönderen: ODTÜ İnsan Araştırmaları Etik Kurulu (İAEK)

İlgi: İnsan Araştırmaları Etik Kurulu Başvurusu

Sayın : Prof.Dr. B.Murat EYÜBOĞLU;

Danışmanlığını yaptığınız yüksek lisans öğrencisi Uygu DEMİRKOL ÇAKMAK' ın "Taşınabilir Tıkayıcı Uyku Apnesi Teşhisi ve İzlenmesi" başlıklı araştırması İnsan Araştırmaları Kurulu tarafından uygun görülerek gerekli onay **2016-FEN-050** protokol numarası ve **01.11.2016-30.04.2017** tarihleri arasında geçerli olmak üzere verilmiştir

Bilgilerinize saygılarımızla sunarız.

Prof. Dr. Canan SÜMER
İnsan Araştırmaları Etik Kurulu Başkanı

Prof. Dr. Melina ALTUNIŞIK
İAEK Üyesi

Prof. Dr. Ayhan SOL
İAEK Üyesi

Prof. Dr. Mehmet UTKU
İAEK Üyesi

Prof. Dr. Ayhan Gürbüz DEMİR
İAEK Üyesi

Yrd .Doç.Dr. Pınar KAYGAN
İAEK Üyesi

Yrd. Doç. Dr. Emre SELÇUK
İAEK Üyesi

BU BÖLÜM, İLGİLİ BÖLÜMLERİ TEMSİL EDEN İNSAN ARAŞTIRMALARI ETİK ALT KURULU TARAFINDAN DOLDURULACAKTIR.

Protokol No: 2016-FEN-097

İAEK DEĞERLENDİRME SONUCU

Sayın Hakem,

Aşağıda yer alan üç seçenekten birini işaretleyerek değerlendirmenizi tamamlayınız. Lütfen "Revizyon Gereklidir" ve "Ret" değerlendirmeleri için gerekli açıklamaları yapınız.

Değerlendirme Tarihi: 12.10.2016

Ad Soyad: Metin girmek için tıklayın

☒ **Herhangi bir değişikliğe gerek yoktur. Veri toplama/uygulama başlatılabilir.**

☐ **Revizyon gereklidir**

- ☐ Gönüllü Katılım Formu yoktur.
- ☐ Gönüllü Katılım Formu eksiktir.

  Gerekçenizi ayrıntılı olarak açıklayınız: Metin girmek için tıklayın
- ☐ Katılım Sonrası Bilgilendirme Formu yoktur.
- ☐ Katılım Sonrası Bilgilendirme Formu eksiktir.

  Gerekçenizi ayrıntılı olarak açıklayınız: Metin girmek için tıklayın
- ☐ Rahatsızlık kaynağı olabilecek sorular/maddeler ya da prosedürler içerilmektedir.

  Gerekçenizi ayrıntılı olarak açıklayınız: Metin girmek için tıklayın
- ☐ Diğer.

  Gerekçenizi ayrıntılı olarak açıklayınız: Metin girmek için tıklayın.

☐ **Ret**

Ret gerekçenizi ayrıntılı olarak açıklayınız: Metin girmek için tıklayın

APPENDIX D

SALTER LABS THERMOCOUPLE DATASHEET

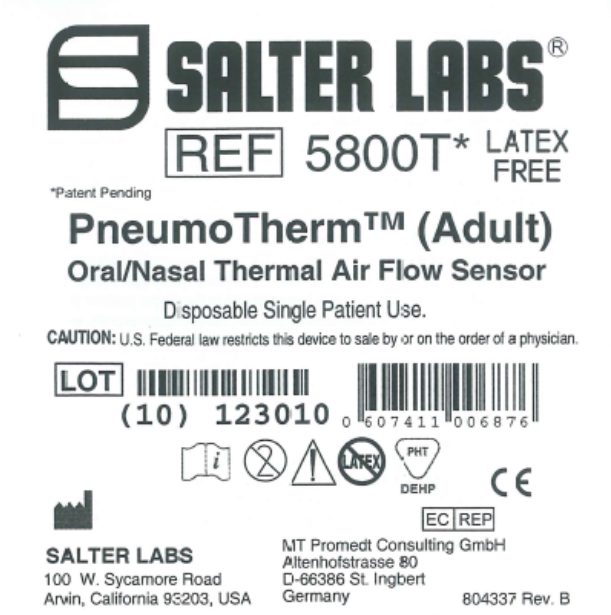

PneumoTherm™ 5800T

System Description: The PneumoTherm Thermocouple (5800T) is designed to interface with the specifically designed Salter Labs Cannulas with patent pending "holder and pocket". When combined, the thermocouple will measure temperature changes in the airflow from the nares and mouth and the cannula will transmit airflow pressure changes from the oral or nasal/oral airflow path to a pressure transducer (BiNAPS® #5500).

General Use: The PneumoTherm Thermocouple (5800T) is inserted into the holder and secured in the pocket of one of the Salter Labs specifically designed cannulas (#5750 & #5751 Nasal or #5760 & #5761 Oral/Nasal). These specifically designed cannulas will position the nasal thermocouple in the proper position in the airflow path. The oral trunk is malleable to position the oral thermocouple in the required oral airflow path away from skin contact. Note: Do Not cut or trim Thermocouple!

Technical Specifications:

Order:	5800T
Cable:	Two conductor white lead wires 2' long
Sensor:	Malleable plastic coated "T" shaped with (2) nasal and (1) oral segment for thermal airflow. Two pin connector to connect to reusable adaptor cable. (Sold separately part # 5810)
Signal Output:	200 uV

APPENDIX E

NELLCOR PULSE OXIMETER DATASHEET

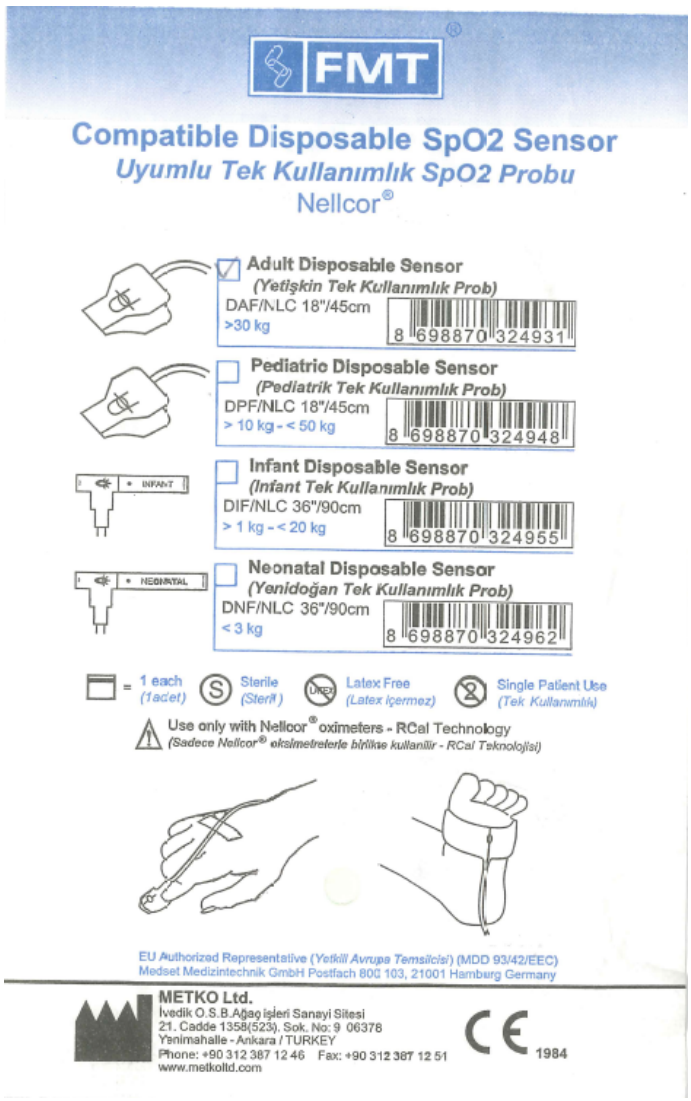

DB-9 Male Connector Pinout Table (Pulse Oximeter Probe Output)	
Pin No	**Signal**
2	Red LED Cathode / IR LED Anode
3	Red LED Anode / IR LED Cathode
5	Photodiode Anode
9	Photodiode Cathode
1-4-6-7-8	Not Connected